EURISOL DS Project
TASK 7: Proton Accelerator design

Deliverable D5

Ion Injector

Layout and beam dynamics report

Planned Date (month): 54

Achieved Date (month): 6/2009

Lead Contractor(s): INFN

Project acronym:	*EURISOL DS*
Project full title:	*EUROPEAN ISOTOPE SEPARATION ON-LINE RADIOACTIVE ION BEAM FACILITY*
Start of the Project:	*1st February 2005*
Duration of the project:	*54 months*

Project funded by European Community under the "Structuring the European Research Area" Specific Programme Research Infrastructures Action within the 6th Framework Program (2002-2006)

Authors:

A. Facco, A. Balabin, F. Scarpa, D. Zenere, INFN-Laboratori Nazionali di Legnaro, Padova, Italy; D. Berkovits, J. Rodnizki, SOREQ, Yavne, Israel; V. Zvyagintsev, TRIUMF, Vancouver, Canada

Abstract

The present document describes the Ion Injector of the EURISOL DS Driver Accelerator. The function of this component is to produce beams of H^-, D^+ and $^3He^{++}$ with specific characteristics for injection in the superconducting linac described in "Deliverable D3-Low and medium beta linac".

The Ion Injector design is the result of beam dynamics studies and search of optimum technological solutions. Reliability and cost-performance considerations have been taken into account in the choice of the components, in a large part already exploited by EURISOL DS participants and contributors.

The Ion Injector layout is described, together with its beam dynamics, the fundamental parameters and characteristics of its components, the main infrastructure requirements, the operation modes, the system performance and the beam losses.

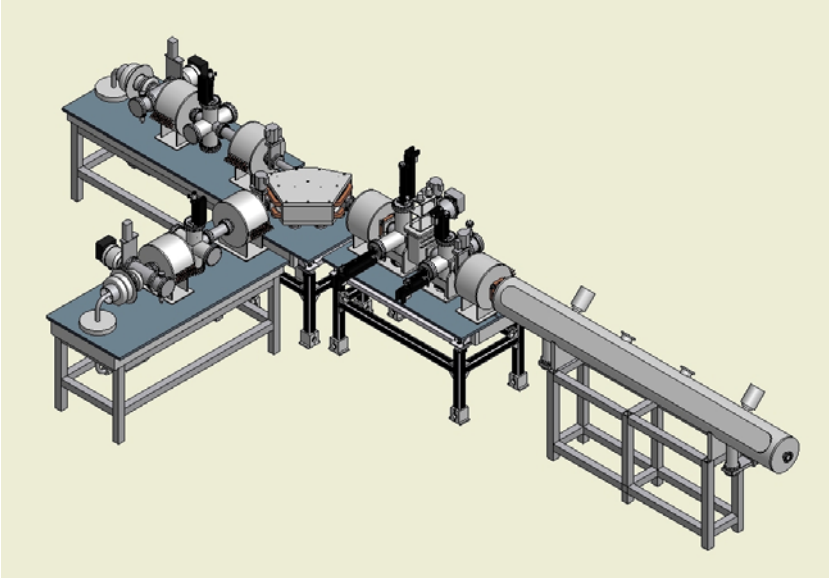

Project funded by European Community under the "Structuring the European Research Area" Specific Programme Research Infrastructures Action within the 6th Framework Program (2002-2006)

1. Introduction

The Ion Injector Section (IIS) is the front end section of the EURISOL Driver Linac (Fig. 1.1) [1]. Its function is the production of H-, D+ and 3He++ beams [14] and their injection in the Low-β section (see Deliverable D3-Low and medium beta linac). It includes the following main sub-sections (Fig. 1.2):

1. H- Ion source
2. ECR source, providing the Deuteron, $^{3}He^{++}$, proton and H_2^{+} beams
3. Low-Energy Beam Transport (LEBT)
4. RFQ

The IIS must provide CW beams with specified intensity, stability and Twiss parameters. It is designed in order to transmit only the part of the beam that will be accepted by the subsequent linac, filtering the particles transmitted, but not accelerated by the RFQ. Most (ideally all) particle losses of the EURISOL Driver will be located in this section and in the MEBT (Medium Energy Beam Transport, part of the Low-β linac described in Deliverable D3), at energy below 1.5 MeV/A.

The IIS design partly resembles the SARAF injector design [2], with important modifications required by the different beam types and the different final energy of the EURISOL driver. The main change is the addition of an H^- source and a straight branch in the LEBT.

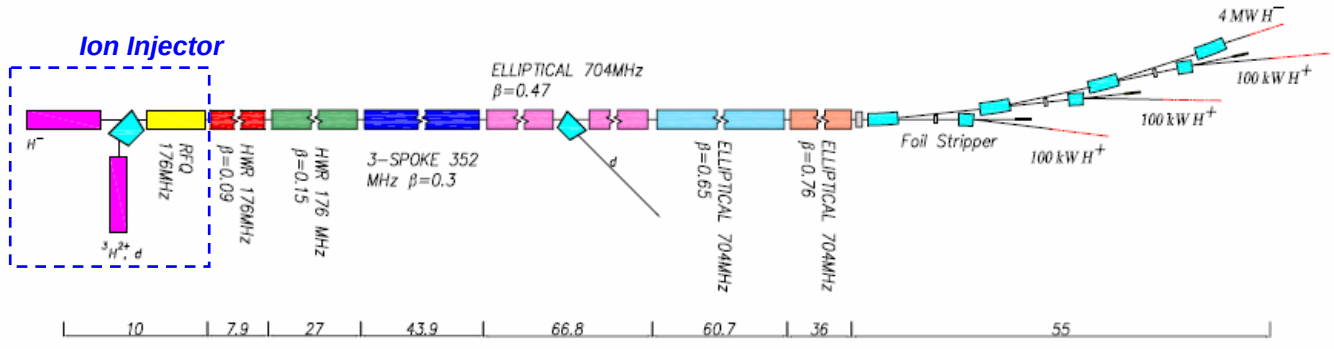

Figure 1.1. Schematic layout of the EURISOL Driver accelerator (not to scale) with the Ion Injector (highlighted in the blue square). The length of the different sections is reported below.

Project funded by European Community under the "Structuring the European Research Area" Specific Programme Research Infrastructures Action within the 6th Framework Program (2002-2006)

The EURISOL IIS has the peculiar characteristic of producing, and accelerating, both negative and positive ions. This puts specific requirements to some of the components, as for the rest of the accelerator. For example, the beam diagnostics must be efficient for both types of beams.

The H^- beam is accelerated in the straight LEBT branch, with the dipole magnet switched off and with no beam mass analysis. This is allowed by the characteristic purity of this beam. The D^+ and $^3He^{++}$ beams (and also H^+ and H_2^+, to be used in the commissioning stage) are accelerated in the 90° branch, that provides sufficient beam selection by means of a set of slits downstream the 90° bending magnet. The beam energy in the LEBT is 20 keV/A. This requires a moderately high extraction voltage for the ECR source, which must reach 40 kV for the Deuteron beam.

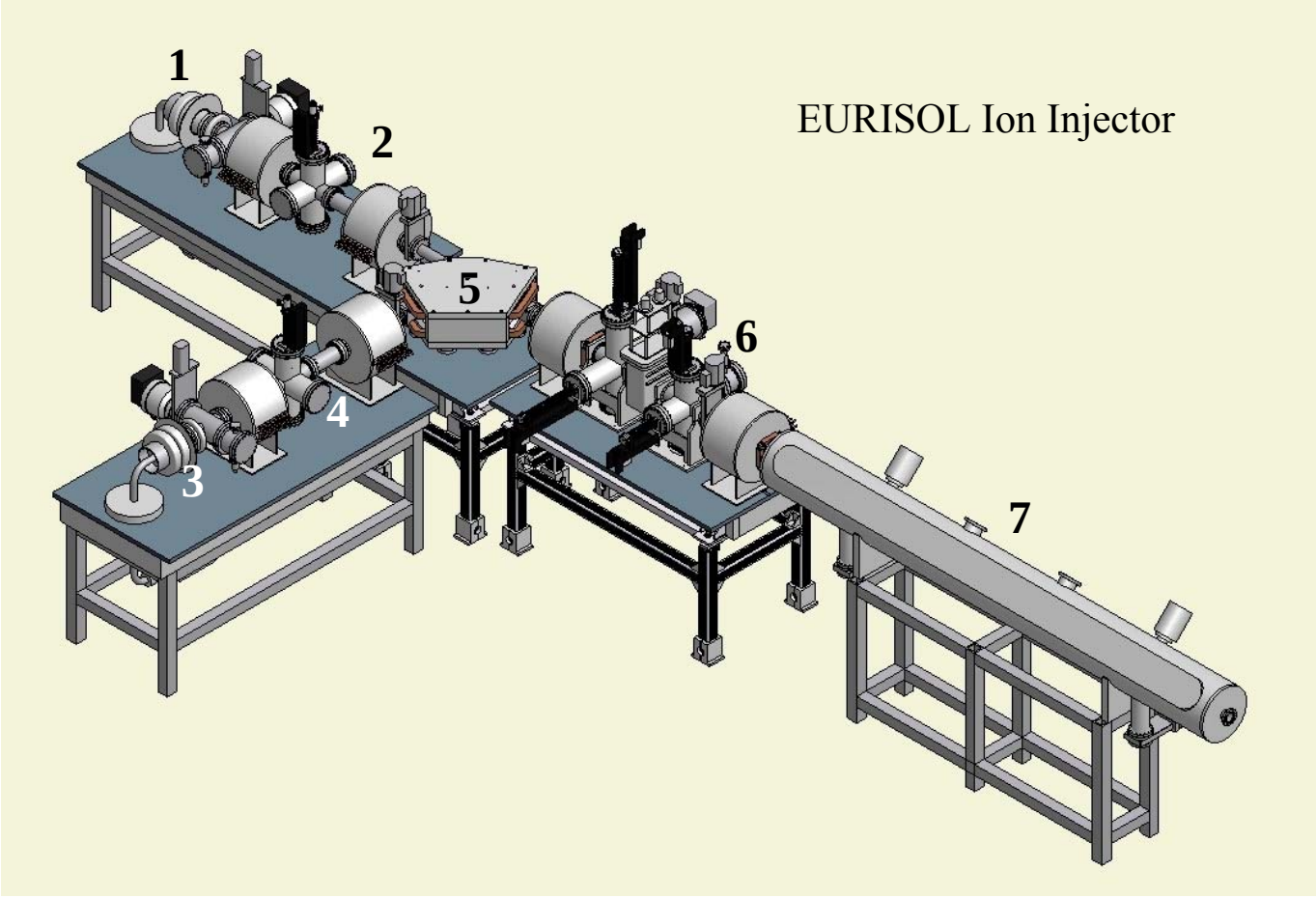

Figure 1.2. 3D view of the EURISOL Ion Injector. 1) multicusp H^- source; 2) H^- (straight) line; 3) ECR D^+, $^3He^{++}$ion source; 4) D^+, $^3He^{++}$ (90°) line; 5) Analysing dipole magnet; 6) common line; 7) RFQ.

The RFQ is similar to the SARAF RFQ [3]. Its nominal transmission is above 90%, fitting the linac

Project funded by European Community under the "Structuring the European Research Area" Specific Programme Research Infrastructures Action within the 6th Framework Program (2002-2006)

requirements. The RFQ output energy of 1.5 MeV/A is sufficient for good transport and acceleration through the following low-β HWR section. Characteristics of this RFQ are good output beam emittance, relatively simple construction and considerably lower cost in comparison to other cw RFQs (IFMIF [15], LEDA [16], TRASCO [17]). This solution was allowed by the maximum beam current of 5 mA required by EURISOL, considerably lower than in other high intensity linac projects (30 to 125 mA).

Although the IIS design is innovative in its capability of accelerating both positive and negative ions, all components proposed for its construction are either commercially available or similar to components which have been already developed and operated by EURISOL participants or contributors. This choice eliminates the risks connected with a dedicated development program.

2. Output beam specifications

The main IIS output beam specifications are listed in table 2.1. These values are dictated by the requirements of the Superconducting Linac input beam. The different timing characteristics are required for the different operation modes which are foreseen.

Table 2.1 Output beam specifications of the EURISOL Driver Ion Injector

Output beams	H^-	D^+	$^3He^{++}$
current (emA)	5	5	0.1
A/q	1	2	3/2
Energy (MeV/A)	1.5		
Bunch Frequency (MHz)	176		
Duty cycle	cw		
Possibility of pulsed operation	Yes		
Pulse length (μs)	>100		
Risetime/falltime (μs)	<20		
Frequency (Hz)	<1000		
Fast shutdown time (μs)	<20		
Output rms emittance (π mm mrad)			
ε_x	<0.2	<0.2	<0.2
ε_y	<0.2	<0.2	<0.2
ε_z	<0.2	<0.2	<0.4
max beam losses total (W)	200	200	30

Project funded by European Community under the "Structuring the European Research Area" Specific Programme Research Infrastructures Action within the 6th Framework Program (2002-2006)

3. Layout and components

3.1 Ion Injector Layout

The IIS layout (shown in fig. 2) includes two injection lines: the 0° (straight) branch, starting from the H^- source, and the 90° branch with the ECR source, both converging to a 90° dipole magnet. Two focusing solenoids are located in each branch between the source and the dipole. A common beam line, including two more solenoids, connects the dipole magnet to the RFQ. An adjustable aperture to control the beam intensity and to cut tails is located just downstream the bending magnet. Movable slits, wire scanners and a Faraday cup to provide measurements of the beam profile, emittance and current are installed between these solenoids. A beam stopper, a diaphragm and an electron suppressor is mounted at the end of the Low Energy Beam Transport (LEBT), in front of the RFQ.

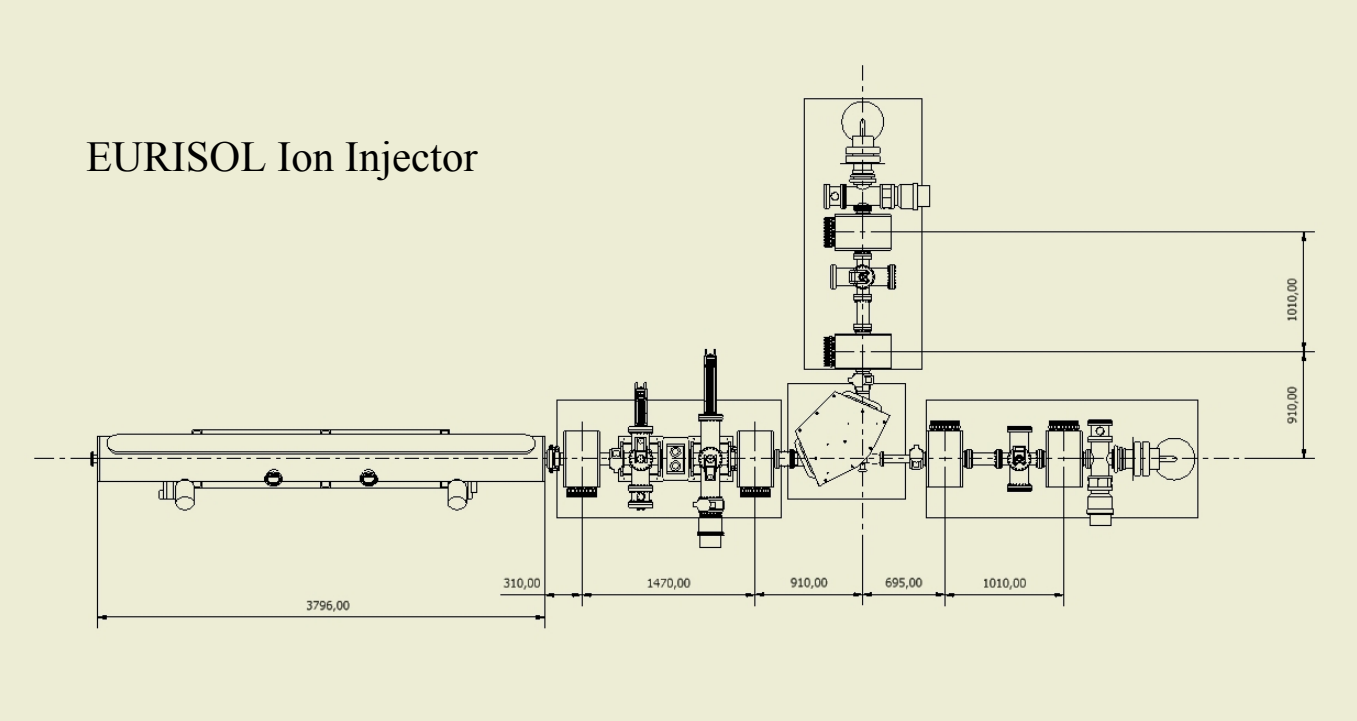

Figure 3.1. Ion Injector Section layout with the main dimensions (in mm) of its components.

Project funded by European Community under the "Structuring the European Research Area" Specific Programme Research Infrastructures Action within the 6th Framework Program (2002-2006)

3.2 Ion sources

3.2.1 H- multicusp Ion Source

The H^- Ion source is a cw multicusp one, similar to the one developed at TRIUMF [4]. This source delivers up to more than 10 mA of H^- beam with normalized rms emittance below 0.125 π mm mrad (see Fig. 3). It can be implemented without difficulties for an extracted beam energy of 20 keV, as required by the EURISOL RFQ. The TRIUMF H^- multicusp is being operated since many years, with high reliability in performance and minimum maintenance requirements.

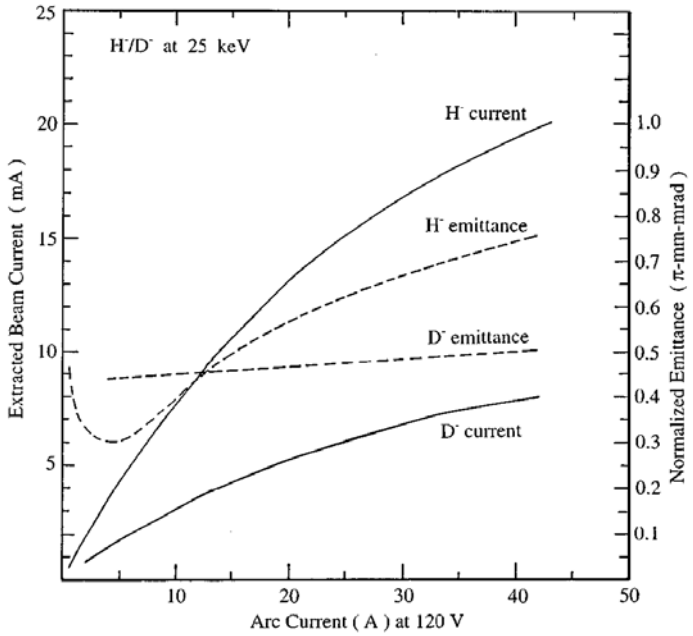

Figure 3.2 Transverse emittance (4 rms normalized) vs. beam current of the H^- and D^- beams of the TRIUMF multicusp source [4].

Table 3.1. TRIUMF and Jyvaskyla [18] H^- cw multicusp sources parameters.

Facility	H^- Beam current	Rep. rate	V extr.	Maintenance interval	Emitt. 90% (norm)	Brightnesss	Power eff.
	mA	Hz	kV	weeks	π·mm·mrad	mA/ $(mm \cdot mrad)^2$	mA/kW
TRIUMF	15	cw	28	~ 6	0.5	3.2	~ 3
Jyvaskyla	3	cw	5.8	~ 6	0.6	1	~ 3

Project funded by European Community under the "Structuring the European Research Area" Specific Programme Research Infrastructures Action within the 6th Framework Program (2002-2006)

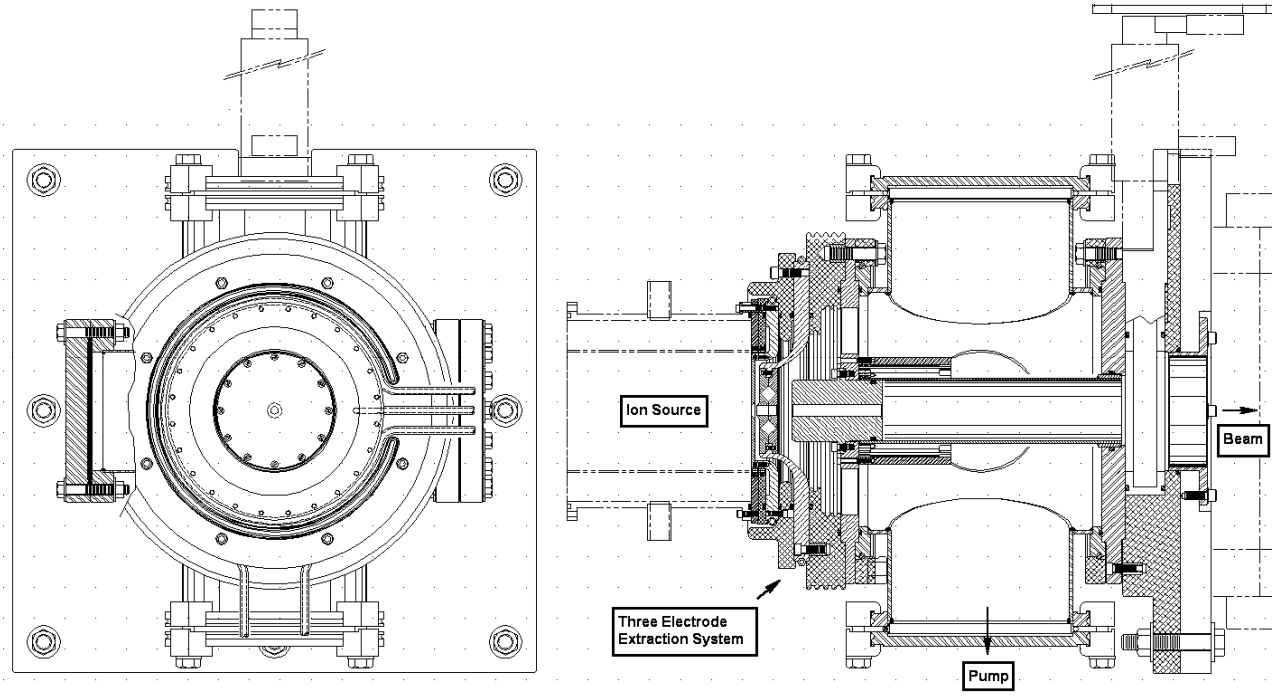

Figure 3.3. TRIUMF H-/D- multicusp source

3.2.2 ECR Ion Source

The $D^+/^3He^{++}$ ion source system is of the type used at SARAF (fig.3.4), which provides the required 6 mA, 20 keV/A deuterons and 200 eμA $^3He^{++}$ ions at a normalized rms emittance of 0.1 and 0.125 π mm mrad, respectively. The SARAF ion source [2] is based on the AECL Chalk River 2.45 GHz ECRIS design [12].

The advantages of an ECR ion source are: ECR generates ions without disposable components such as cathodes or filaments. This easies and stabilizes the operation and increases the time between maintenances. The ionization efficiency of an ECR is high. This parameter becomes important when using an expensive gas such as ^3He.

Several changes have been made by ACCEL [13] regarding the original design. The extraction geometry was adjusted to the required maximum current, the RF vacuum window in the RF wave guide was moved in front of a 90° bent to avoid damages by electrons and a solid boron nitride plate has been installed

Project funded by European Community under the "Structuring the European Research Area" Specific Programme Research Infrastructures Action within the 6th Framework Program (2002-2006)

between wave guide and plasma chamber to prevent the plasma from entering the wave guide (fig.3.4). Furthermore the wave guide is pumped by an additional bypass.

The plasma is confined using two solenoids run by a 125 A power supply. Typical RF power for analyzed 5 mA deuterons is 800 W. For this current the D_2 gas flow is 0.38 sccm. The extraction electrode voltage is 40.0 kV and the deceleration electrode, which is used to prevent electrons for entering the plasma, is tuned around -1 kV, to optimize beam properties. The high voltage power supply current is typically 8.5 mA which means that about 60% of the extracted current is the elemental ion d and the rest are molecules; D_2^+ and D_3^+. The ECR plasma temperature is about 1-3 eV. The ECRIS temperature, the plasma instabilities, the extraction aperture size (diameter = 2.5 mm) and the extraction electrode geometry define the initial beam quality.

The beam parameters are measured in the LEBT and reported in the next section.

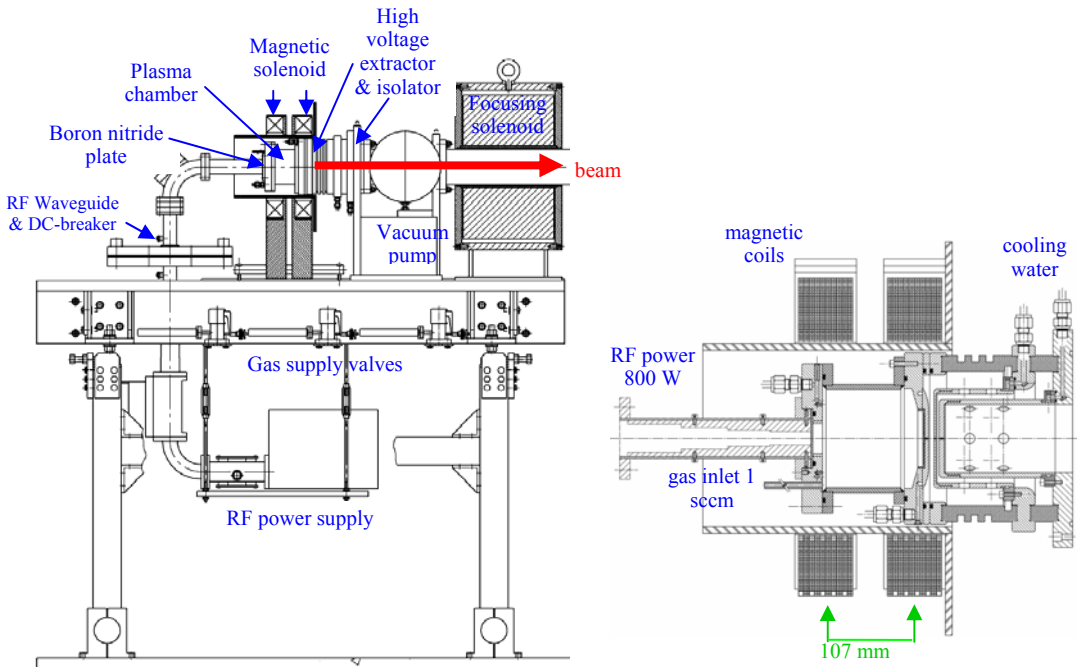

Figure 3.4. The SARAF ECR ion source [2][13]. The drawings in the right side present in details the plasma chamber vicinity.

Project funded by European Community under the "Structuring the European Research Area" Specific Programme Research Infrastructures Action within the 6th Framework Program (2002-2006)

Table 3.2. ACCEL ion source main parameters [2,13]

Parameter	***Specification***
ION SPECIES	p, d, H_2^+, $^3He^{++}$
Extraction Energy	20 keV/u
Energy ripple	±0.03 keV/u
Current range	0.04 – 5 mA (0.2 mA for $^3He^{++}$)
Current ripple (max current)	±2 %
Transverse emittance (norm, r.m.s.) (measured at the LEBT)	0.2 π·mm·mrad

3.3 LEBT

The LEBT includes a double-focusing 90° dipole magnet with 500 mm curvature radius and 23.6° edge angles. Two beam lines, one for each ion source, are converging on it; a common line is bringing the beam from the dipole to the RFQ. The dipole ensures an efficient separation of the nominal $D^+/^3He^{2+}$ beams from their main pollutants (D_2^+, $D_3^+/^3He^+$). The specific feature of the Lines 1 and 2 (fig. 2) is the use of 4 solenoids for beam matching into the RFQ. This layout allows good matching in a wide range of input beam parameters and ion species. The given input and the required output beam parameters of the Eurisol LEBT lines are listed in Table 3.3.

Table 3.3. LEBT and RFQ input beam parameters.

Ions	W, keV	W, keV/u	I, mA	Input			Output (RFQ input)		
				α	β, mm/mrad	$\varepsilon_{n,rms}$ π·mm·mrad	α	β, mm/mrad	$\varepsilon_{n,rms}$ π·mm·mrad
H^-	20	20	6.3	-4.344÷0	0.332	0.125	1.313	0.0418	<0.2
D^+	40	20	5.6	-5.43÷0	0.415	0.1	1.224	0.0398	
$^3He^{2+}$	60	20	0.11	-4.344÷0	0.332	0.125	1.151	0.0379	

Project funded by European Community under the "Structuring the European Research Area" Specific Programme Research Infrastructures Action within the 6th Framework Program (2002-2006)

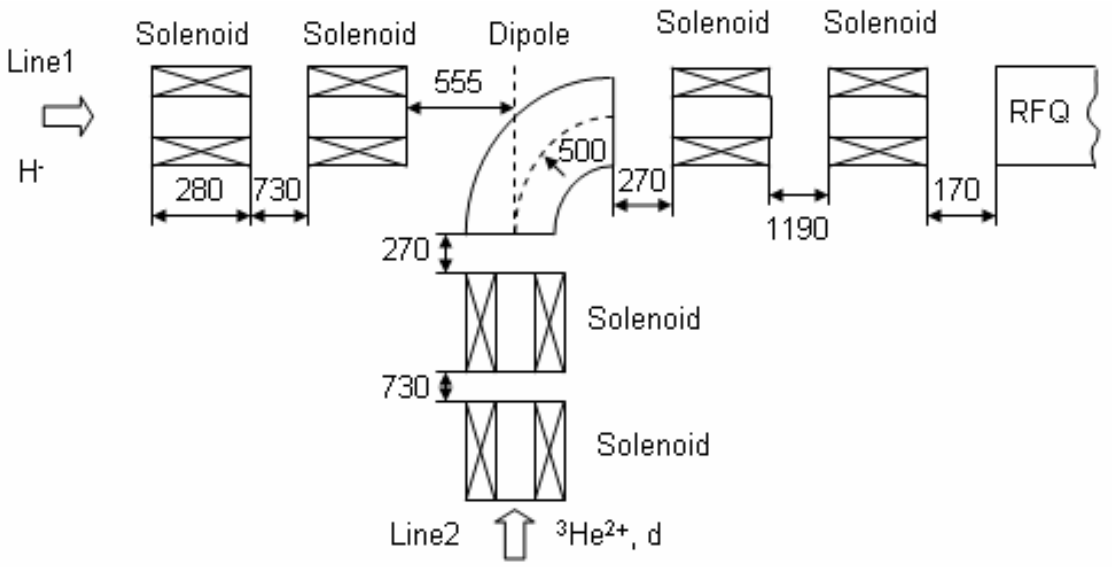

Figure 3.5. LEBT schematic layout.

The chosen input parameters, at the given emittance, correspond to a beam rms radius of 2.5 mm and divergence of 0÷33 mrad. Different α and β values, that depend on the specific extraction geometry of the source, can be handled by the optical system. Along the LEBT lines it is assumed that the nominal H^- and $D^+/^3He^{2+}$ beams have a space charge compensation of 80%, except for the bending magnet in Line 2 (fig.2) where the space charge compensation is cancelled by the dipole magnetic field. This value was assumed as a conservative one according to reff. [6],[7],[8]. The LEBT design is based on the SARAF

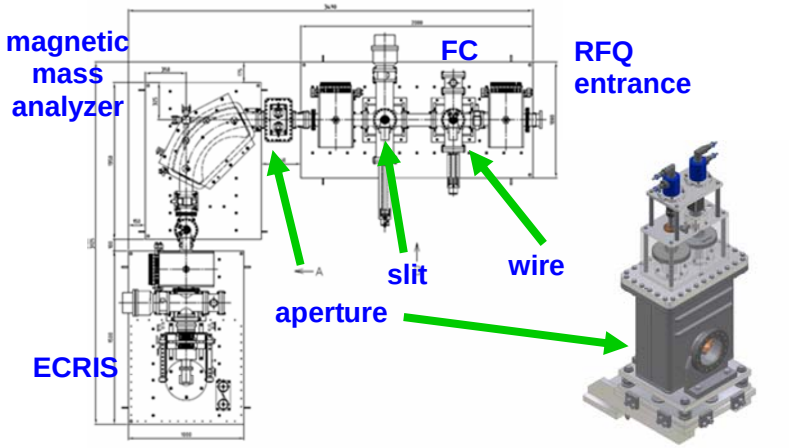

LEBT design (fig. 3.6). Typical beam parameters measured at SARAF LEBT are presented in table 3.4.

Project funded by European Community under the "Structuring the European Research Area" Specific Programme Research Infrastructures Action within the 6th Framework Program (2002-2006)

Figure 3.6: The SARAF LEBT

Table 3.4. Positive ion source beam parameters

Parameter Unit specified Value	units	H+	H_2^+	D+
Maximum beam current	mA	5	5	5
Beam current spread [rms]	%	4 @ 5 mA	4 @ 5 mA	4 @ 5 mA
Beam current stability [p-p]	%	+/-2.5 @ 5mA	+/-2.5 @ 5mA	+/-2.5 @ 5mA
Beam current adjustment accuracy	mA	0.1 @ 5 mA	0.1 @ 5 mA	0.1 @ 5 mA
Extraction energy	keV/nucleon	20	20	20
Extraction energy spread [rms]	eV/nucleon	+/- 30	+/- 30	+/- 30
Extraction energy stability [p-p]	eV/nucleon	+/- 30	+/- 30	+/- 30
Normalized rms emittance x/y	π mm mrad	0.2/0.2	0.2/0.2	0.2/0.2

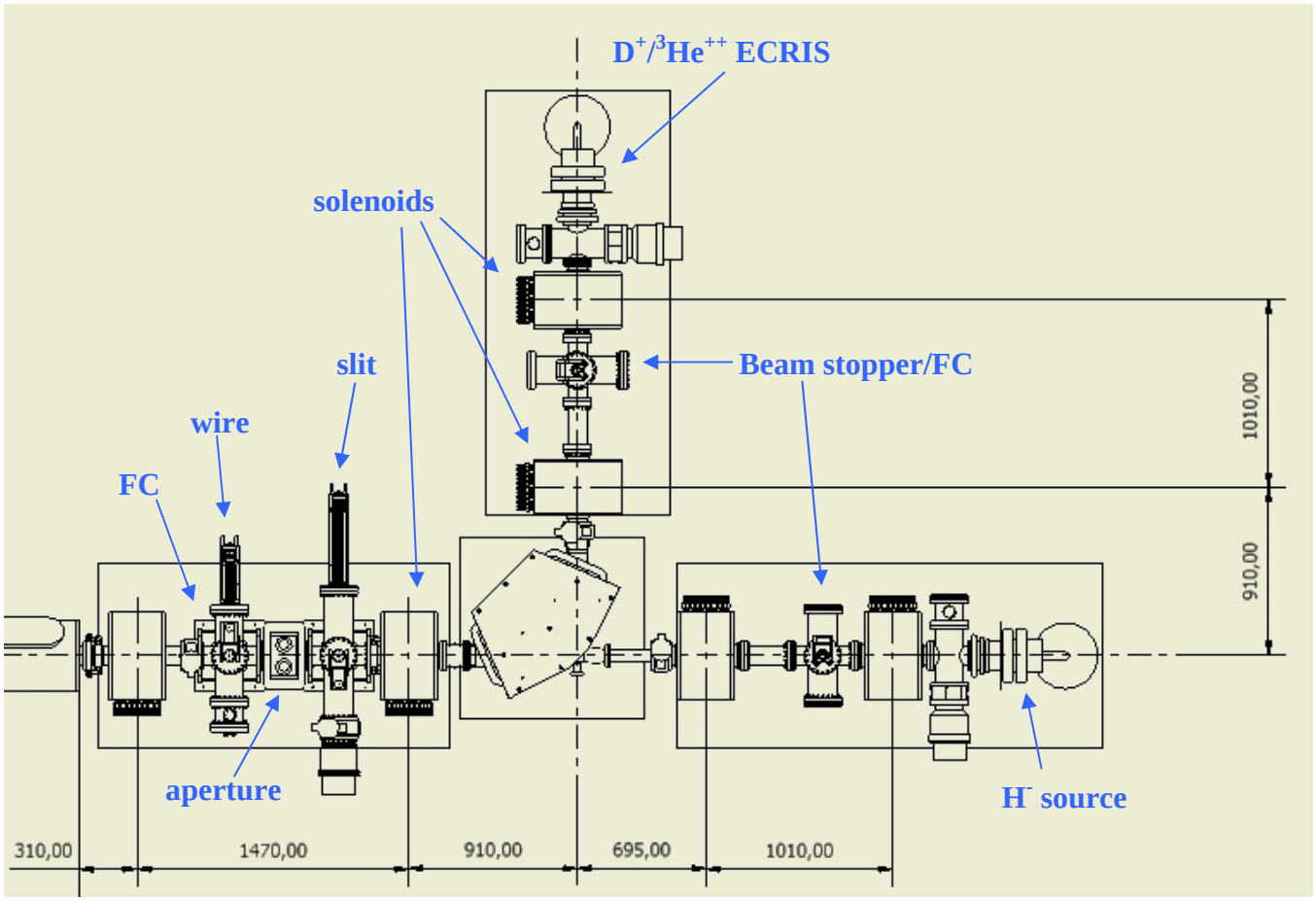

Project funded by European Community under the "Structuring the European Research Area" Specific Programme Research Infrastructures Action within the 6th Framework Program (2002-2006)

Fig. 3.6. The EURISOL LEBT main components.

The commom branch of the LEBT includes a slit-wire system for beam profile and emittance measurement, a Faraday cup for beam current measurement, and a variable aperture for beam A/q selection.

The straight and the 90° branches of the LEBT are similar, each including a beam stopper-Faraday cup. Each line is equipped with beam steerers.

To prevent injection of a significant current of e^- in the RFQ, a diaphragm-suppressor is placed at the LEBT end. This suppressor is of the type described in ref. [9], requiring about -1.5 kV bias voltage. The aperture diameter is 4.5 mm.

Table 3.5. LEBT Magnetic elements characteristics

Element	units	Dipole	Solenoid	Steerers
Length	mm	-	280	100
Total aperture	mm	60	80	80
Max. field B	T	0.1	0.33	-
Max field Integral	T·m	-	0.1	10^{-4}
Bending radius	mm	500	-	-
Bending angle	deg	90	-	-
Edge angle	deg	23.6	-	-

Beam stoppers - Commercial, water cooled beam stoppers are located in each of the two injector branches, between the first and the second solenoid. These stoppers are used also as Faraday Cups (FC).
Beam steerers - A couple of horizontal and vertical magnetic steerers are located after each of the LEBT solenoids for beam angle correction. Suitable steerers are standard, air cooled ones, with maximum field integral $B=l\cdot10^{-4}$ T·m. The steeres are operated with a Delta 30V x 5 A dual polarity power supply but in usual operation the steeres current do not exceed 1 A.
Slits - Vertical and horizontal, remotely controlled water cooled slits are located between the two solenoids downstream the 90° bending magnet emittance measurement (together with diagnostics box IIS 1). A variable aperture diaphragm is also available for beam analysis and beam current regulation.

Project funded by European Community under the "Structuring the European Research Area" Specific Programme Research Infrastructures Action within the 6th Framework Program (2002-2006)

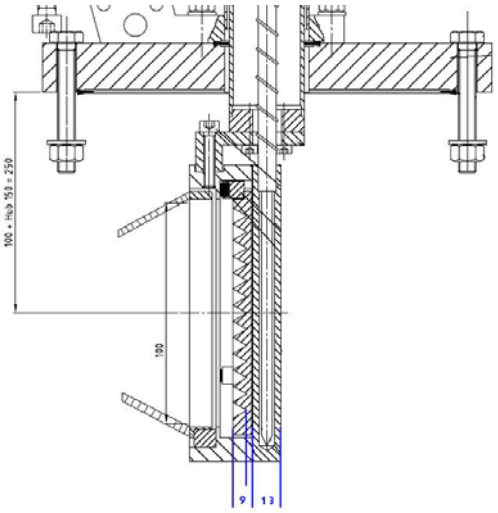

Figure 3.7: A cross section of the LEBT Faraday Cup. The FC is retractable with a dynamic range span of 4". The cup surface is made of teethed 9 mm thick graphite plate backed by a 13 mm thick water cooled copper plate. The suppressor is charged by -300 DC V. The suppressor opening is 70 mm. The cup is designed to safely hold 200 W. The cup is fabricated by Accel-RI.

3.4 Diagnostics

The IIS diagnostics includes a box, located between the two solenoids before the RFQ and containing a wire scanner and a Faraday cup (water cooled for a 200 W beam). This box allows to monitor beam current, beam shape, to measure beam phase space and emittance (together with a set of movable slits).

3.4 RFQ

The 4-rod, 176 MHz cw RFQ can be similar to the one installed in SARAF [10]. This RFQ is characterized by a relatively small size and moderate construction cost, and can provide output beams with good emittance characteristics. Its nominal transmission, although not extremely high, is more than sufficient for the present application. The beam power losses are rather modest due to the relatively low energy of the lost particles. According to calculations, the transmitted, but not accelerated particles are well separated in energy from the accelerated ones and they can be efficiently stopped in the following MEBT with low power losses (within a few Watts).

The maximum power required to reach the voltage for deuteron acceleration is about 250 kW. The maximum beam loading (15 kW for 5 mA beams) is always low compared to rf losses.

At present, the SARAF RFQ is undergoing commissioning, thus in principle the reliability of this rather convenient solution is not yet demonstrated. If the SARAF RFQ performance will not reach completely its design goal, the design and construction of a longer RFQ with larger safety margins on power density

Project funded by European Community under the "Structuring the European Research Area" Specific Programme Research Infrastructures Action within the 6th Framework Program (2002-2006)

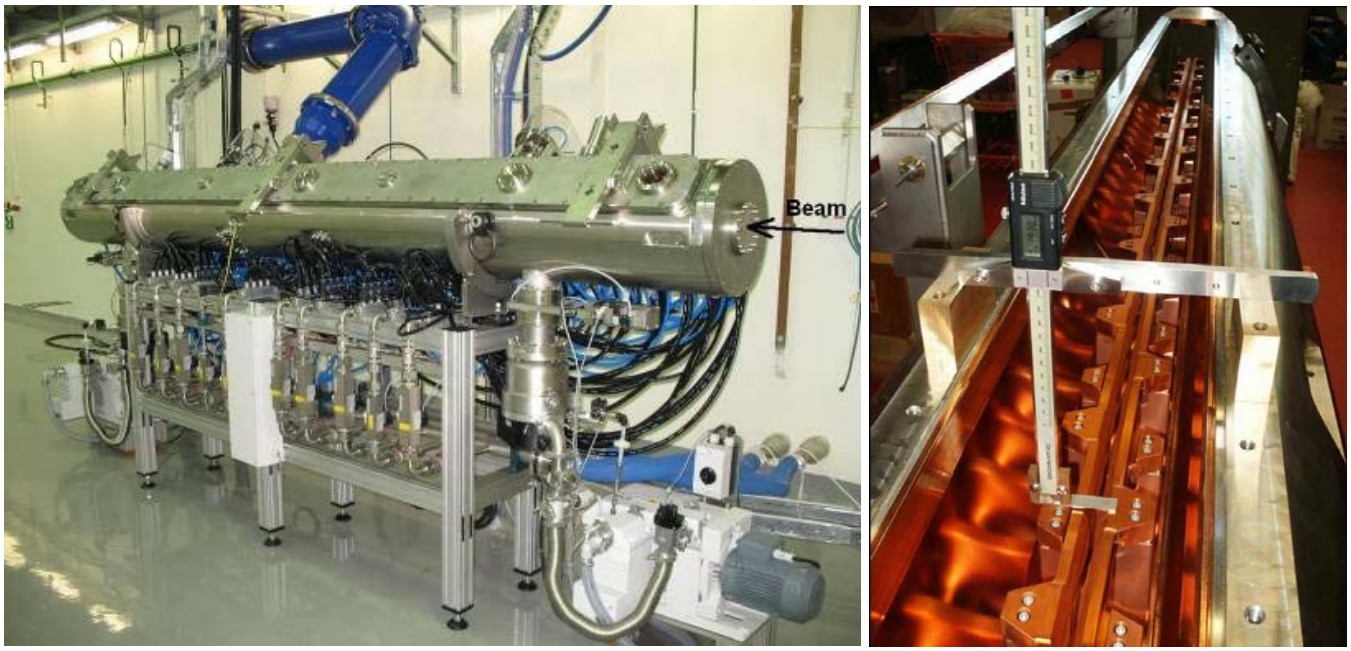

Figure 3.8 View of the SARAF RFQ. Right: RFQ interior during assembly [10].

Table 3.8. SARAF RFQ parameters.

Injection/output energy	20 / 1500 keV/u
Isotope A/q	≤2
Frequency	176 MHz
electrode voltage	65 kV
RFQ length	3.8 m
inner diameter	280 mm
min. aperture	2.7 mm
max. modulation	2.7
power consumption	250 kW
input emittance *x,y*	160 π mm mrad
a / b	0.85/0.28 mm mrad^{-1}
number of cells	199
number of stems	40
long. output emittance ε_l	75 π deg. keV/u
transmission 0 / 5mA	98 / 96 %
Quality factor	3750
Rf power consumption max.	250 kW
Peak surface electric field	~1.6 Kilpatrick

and peak fields appears to be a realistic alternative with low risk, although with higher cost. A possible

alternative would be the construction of an RFQ with the same electrodes profiles, buth with a 4-vane structure, which is considered more reliable for cw operation. A similar RFQ would have dimensions and power requirements close to the SARAF RFQ ones, and the same beam dynamics behavior, although at the price of a higher construction cost. A suitable 4-vane structure for cw operation at a similar frequency (175 MHz) is under construction for the IFMIF-EVEDA project [15].

Project funded by European Community under the "Structuring the European Research Area" Specific Programme Research Infrastructures Action within the 6th Framework Program (2002-2006)

4 Beam dynamics

The IIS beam dynamics was studied with the TRACEWIN code developed at CEA Saclay [11].

4.1 Design criteria

The main design guidelines of the IIS structure were:

- good output beam quality (rather than highest transmission);
- beam losses confined mainly at low energy;
- low construction and operation cost;
- low technological risk.

The EURISOL driver accelerator must deliver both positive and negative ion beams. The IIS must provide both types of beams accelerated in the same RFQ. This requires two different types of ion sources and two distinct injection lines. The line for D^+ and $3He^{++}$ beams, rich of contaminants, requires a dipole magnet for beam analysis. The H- line, thanks to the purity of this beam, does not require beam analysis, and can be made without bends. Both lines contain 2 solenoids before the 90° dipole magnet to allow ideal matching for all required beams. Solutions with only one solenoid in that section were also explored; however, we chose the 2 solenoid solution because it made easier and more reliable the line optimization in a wide range of input beam parameters with a modest cost increase.

The choice of the SARAF-type RFQ (either 4-rod or 4-vane) was motivated by the following considerations:

- The relatively low injection energy (20 keV/u), that allows a short RFQ bunching section, and the relatively low output energy (1.5 MeV/u) make this RFQ rather short, compared to other ones for high current, cw protons and deuterons. Its construction is relatively simple and cost effective.
- The output beam energy of 1.5 MeV/u resulted to be sufficiently high for injection in a 176 MHz linac made of superconducting HWR cavities and superconducting solenoids. The cost of this linac, per MeV of acceleration in cw mode, is significantly lower than the same cost for RFQ structures; this calls for a short RFQ.
- The beam transmission of the SARAF RFQ is above 90% for all required beams. Although other RFQ structures (e.g. IFMIF RFQ, designed for a 125 mA D beam) could reach higher transmission, in

Project funded by European Community under the "Structuring the European Research Area" Specific Programme Research Infrastructures Action within the 6th Framework Program (2002-2006)

the SARAF RFQ particles are lost mostly at low energy. As a result, the cavity activation is rather low and the beam power losses are negligible (below 1 kW) in comparison with the rf power losses in the resonator walls.

- The nominal output beam emittance of the RFQ is satisfactory and comparable to the present state of the art.
- The rf power and cooling requirements of the SARAF RFQ are much lower than in other cw RFQs (LEDA, TRASCO, IFMIF).

All these aspects make the SARAF RFQ perfectly adequate to the EURISOL requirements.

4.2 Space charge compensation

High current beams of light ions are characterized by strong space charge forces, that would cause very high field magnet and induce very compact line which would be incompatible with diagnostics insertion in the absence of a neutralisation mechanism deriving from ionization of the residual gas in the beam lines [6][20]. This mechanism acts both for positive and negative ions. The neutralization effect depends on the residual gas pressure, and the characteristic time required for it to stabilize is of the order of a few tens microseconds for a residual pressure around 10^{-5} hPa [7]. In the normal IIS operation with cw beam, a stable neutralization is expected. In the pulsed mode, the beam pulse length must be kept longer than this characteristic time.

Neutralization is largely cancelled in dipole bending magnets, which bend positive and negative charges in opposite directions, away from the beam trajectory. In focusing solenoids, on the contrary, the magnetic field contributes to maintain the neutralizing charge along the beam [7].

Self-consistent codes for space charge compensation calculations are under development at CEA [19], but not yet usable for our scope. However, the results that can be found in literature suggest that a large compensation is always present in normal conditions. In the EURISOL injector calculations, the compensation factor of 80% was used. This is the same value used for the beam dynamics calculations of the SPIRAL2 injector, characterized by 5 mA deuteron beams as the EURISOL IIS [8]. We assume that compensation factors even larger than 80% should apply in the real IIS accelerator conditions, and that successful beam transport with the same output beam parameters should be obtained with a slightly different tuning of the beam line.

Project funded by European Community under the "Structuring the European Research Area" Specific Programme Research Infrastructures Action within the 6th Framework Program (2002-2006)

4.3 Multiparticle simulations

4.3.1 LEBT lines

Beam dynamics simulations of the Eurisol LEBT lines with realistic magnetic fields inside the solenoids (fig.4.1) were performed by means of the TraceWin/Partran package.

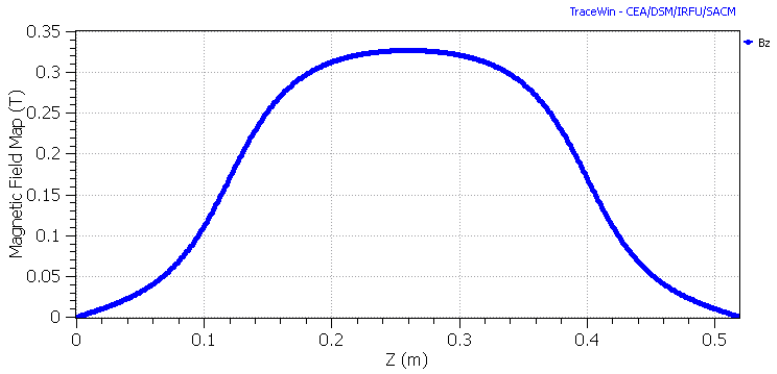

Fig. 4.1. Magnetic field distribution along the beam axis of the LEBT solenoids (aperture radius=40mm; Length =280mm).

A goal of the simulations was to determine a focusing solenoids configuration in the LEBT lines that provides full beam matching with a RFQ by only changing the magnetic fields in the solenoids. The envelope code TraceWin was used to find the preliminary values of the magnetic fields. Then the multiparticle code Partran was applied to calculate realistic output beam parameters and to correct the focusing strength. An initial Gaussian distribution of 100000 macroparticles was used for the final Partran simulation of the LEBT lines. This distribution was truncated at 4σ at the source exit.

4.3.1.1 Line 1 (H^-)

To limit the potential losses in the RFQ, a diaphragm with 2.25 mm aperture radius was located at RFQ input. The nominal H^- current at the source exit was set at 6.3 mA. The space charge compensation factor of 80% was assumed along the all line up to the RFQ, including the dipole magnet which is of course

Project funded by European Community under the "Structuring the European Research Area" Specific Programme Research Infrastructures Action within the 6th Framework Program (2002-2006)

switched off when the H- beam passes through it. The remaining input beam parameters are set to the values listed in Table 3.3. The input phase spaces corresponding to the divergent H^- beam are shown in fig.4.2. The R-Z space charge model was utilized [11] for the simulation of this axially symmetric line. Space charge forces were calculated by the 2D PICNIR subroutine on a 50x50 mesh.

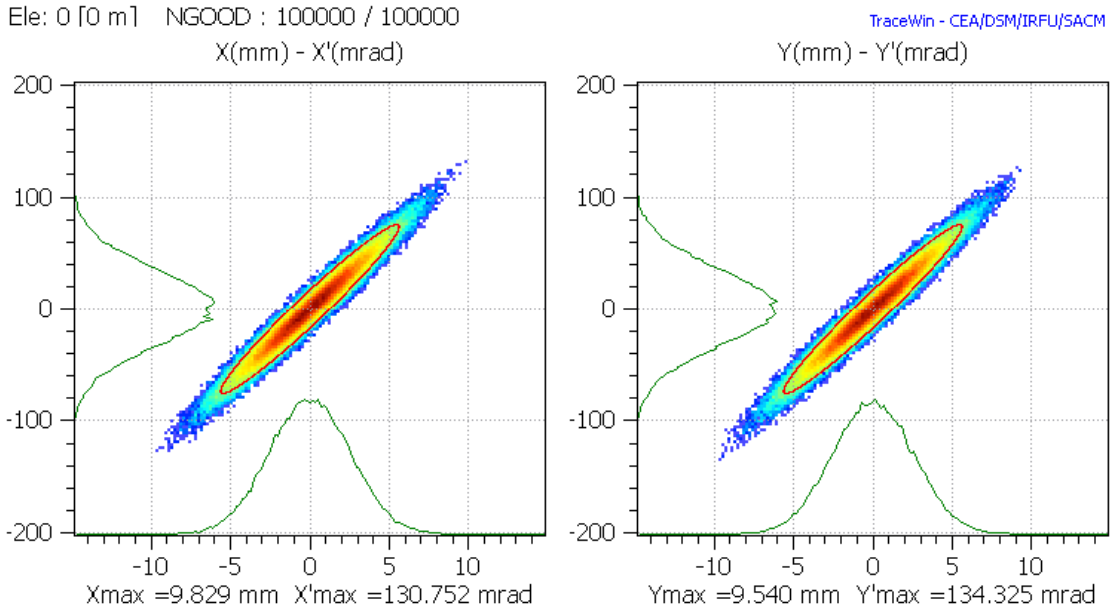

Fig. 4.2. LEBT H^- input phase spaces for α=-4.344; β=0.332 mm/mrad and $\varepsilon_{n,rms}$=0.125 π·mm·mrad

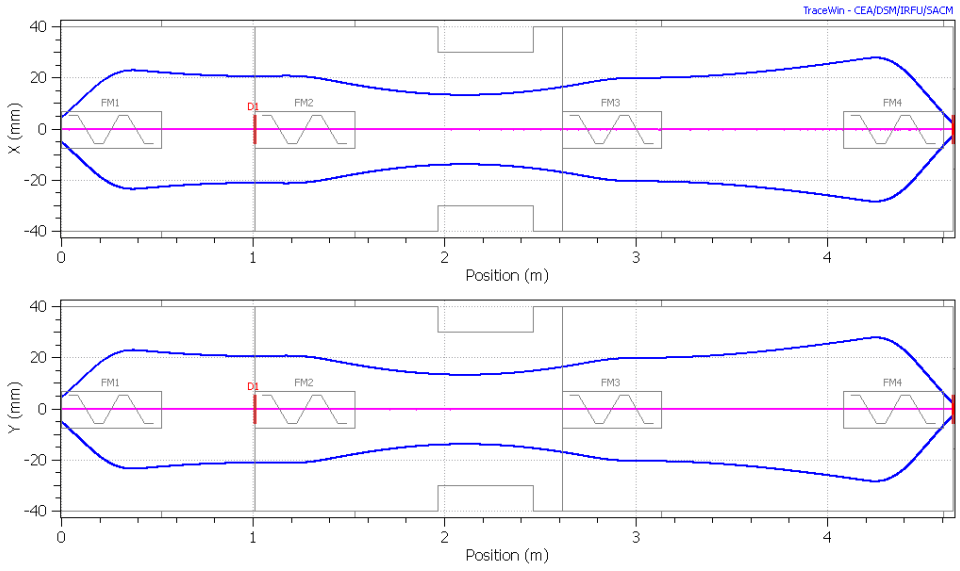

Fig. 4.3. H^- envelopes (2 rms) in the Line 1 (straight).

Project funded by European Community under the "Structuring the European Research Area" Specific Programme Research Infrastructures Action within the 6th Framework Program (2002-2006)

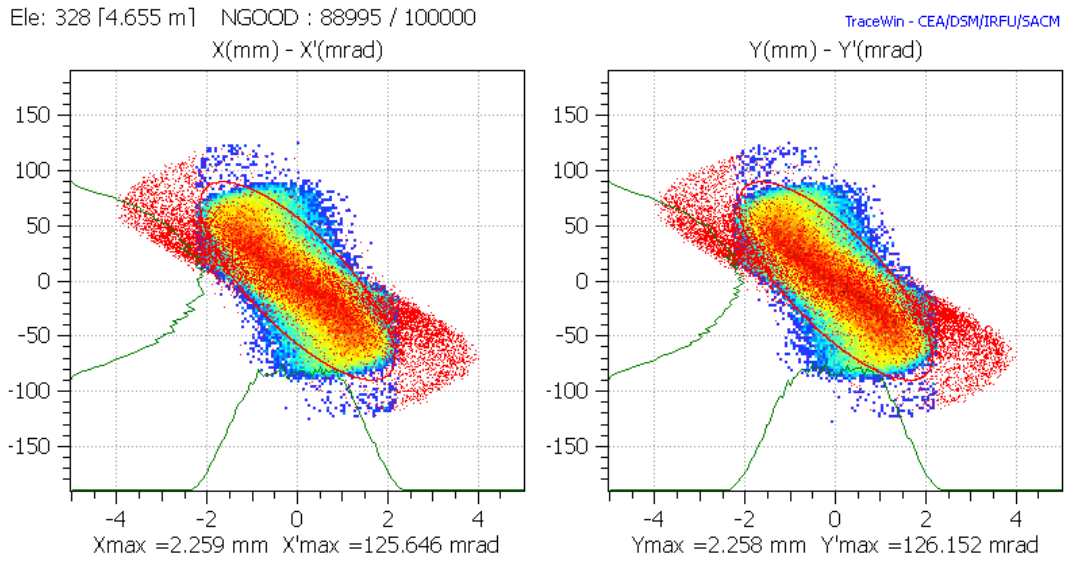

Fig. 4.4 H^- output transverse phase spaces at the diaphragm-suppressor (RFQ input). Particle lost in the diaphragm are plotted in red in the figure.

The calculated transmission in the H^- LEBT line is about 89%. Particle losses of about 12 W mainly take place at the diaphragm. The output normalized rms emittances are estimated to be $\varepsilon_{nx,rms}=\varepsilon_{ny,rms}=0.171$ π·mm·mrad, and the output Twiss parameters are close to the matched values at RFQ input (Table 1).

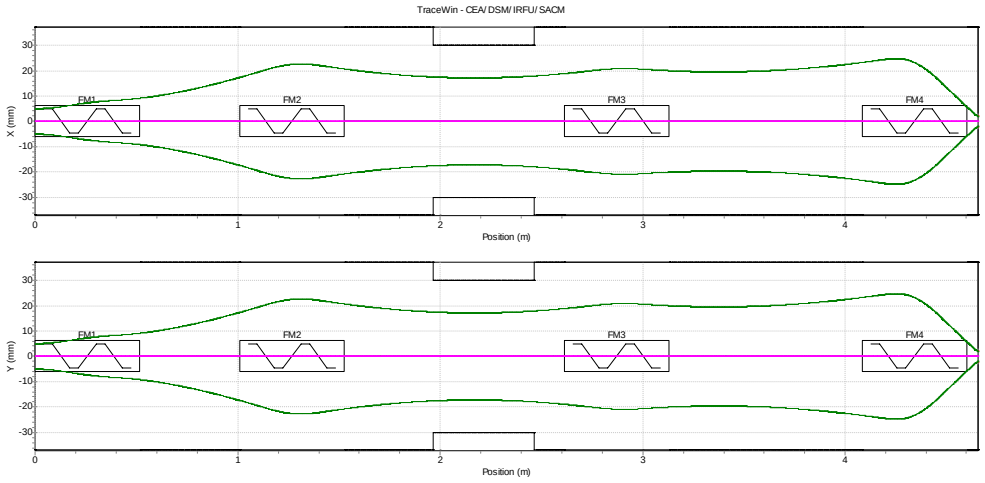

Fig. 4.5. Example of H^- envelopes in the Line1, matched to the RFQ with an input beam with Twiss parameters significantly different from the nominal ones.

Project funded by European Community under the "Structuring the European Research Area" Specific Programme Research Infrastructures Action within the 6th Framework Program (2002-2006)

The 4 solenoids design allows full beam matching into the RFQ for a wide range of beam parameters at the source exit. The line was simulated also with different values of the input beam Twiss parameters, reaching the same reults (see fig.4.5).

4.3.1.2 Line 2 ($D^+/^3He^{2+}$)

In the D^+ and $^3He^{2+}$ beams simulation in the LEBT Line2 (the 90° line in fig. 3.5), space charge compensation was assumed to disappear in the bending magnet, where the compensating electrons are scattered by the dipole magnetic field. The nominal currents of D^+ and $^3He^{2+}$ beams at the source exits were set at 5.6 mA and 0.11 mA, respectively. The remaining input beam parameters were set to the values listed in Table 3.3. The input D^+ and $^3He^{2+}$ phase spaces, corresponding to divergent beams, are very similar to the H^- phase spaces shown in fig. 4.2.

Edge angles of 23.6° were chosen for the dipole magnet. This value, obtained with an optimization process, is a compromise for minimum emittance growth caused both by space charge effects in the dipole and nonlinear phase space distortion in the edge.

For this simulations the X-Y-Z space charge model was utilized. Space charge forces were calculated by the 3D PICNIC subroutine on a 9x9x9 mesh. Simulation results are presented in the following figures.

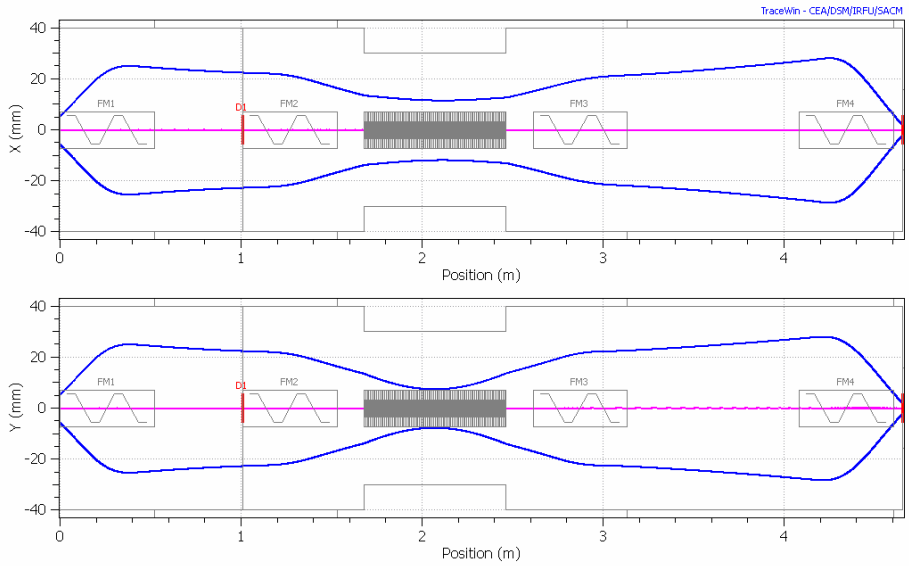

Fig. 4.6. Deuteron envelopes in Line 2 (90°).

Project funded by European Community under the "Structuring the European Research Area" Specific Programme Research Infrastructures Action within the 6th Framework Program (2002-2006)

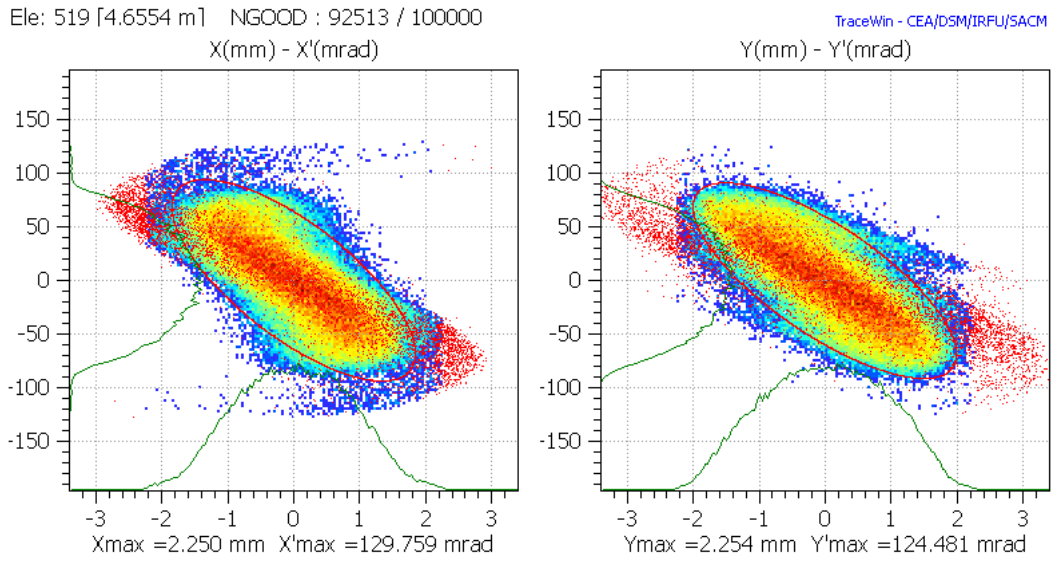

Fig. 4.7. Deuteron output transverse phase spaces at the diaphragm-suppressor (RFQ input). Particle lost in the diaphragm are plotted in red in the figure.

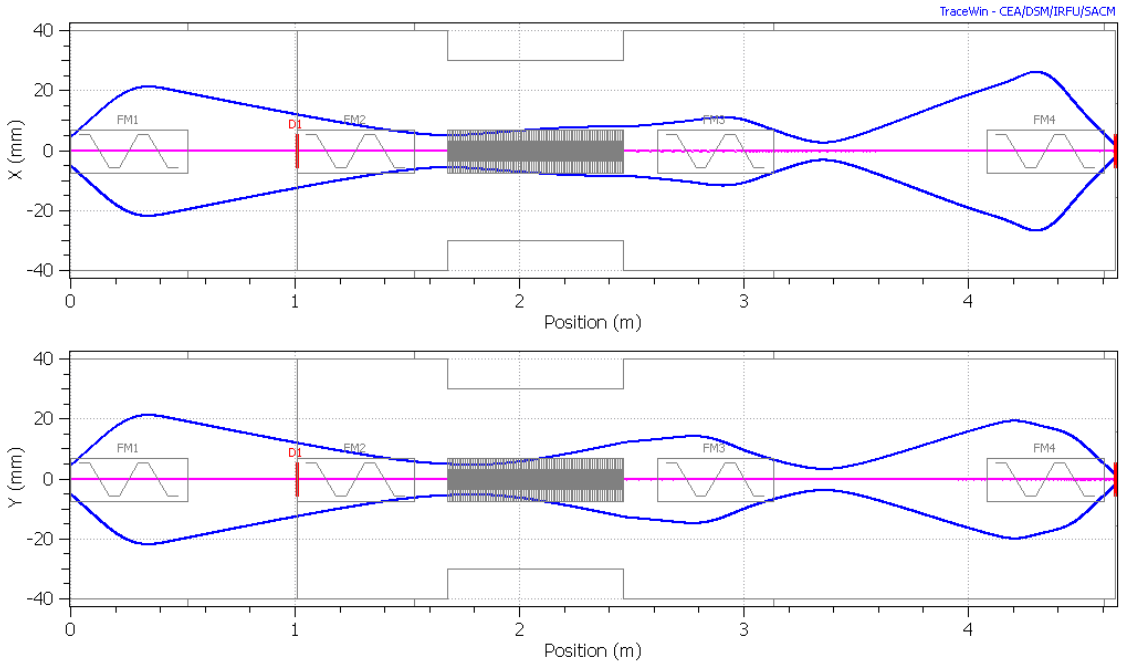

Fig. 4.8. $^{3}He^{2+}$ envelopes in the Line2

Project funded by European Community under the "Structuring the European Research Area" Specific Programme Research Infrastructures Action within the 6th Framework Program (2002-2006)

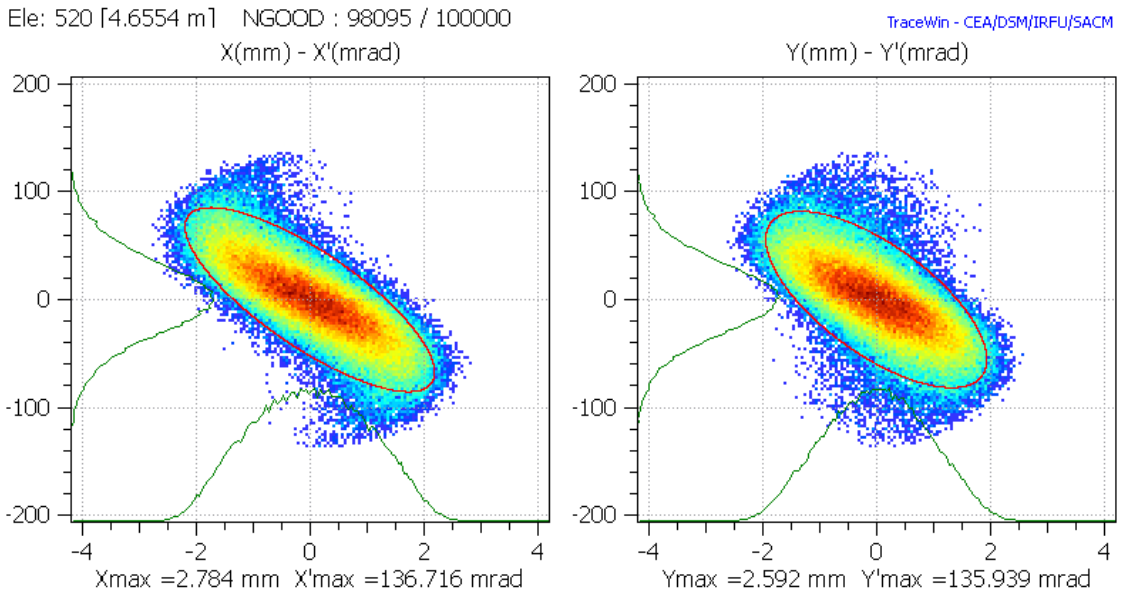

Fig. 4.9. $^{3}He^{2+}$ output phase spaces

The transmission is about 98% for D^{+} and for $^{3}He^{2+}$ in the Line2 before the diaphragm.

The output normalized rms emittances are estimated to be $\varepsilon_{nx,rms}$=0.155 π·mm·mrad $\varepsilon_{ny,rms}$=0.155 π·mm·mrad for D^{+} and $\varepsilon_{nx,rms}$=0.150 π·mm·mrad $\varepsilon_{ny,rms}$=0.152 π·mm·mrad for $^{3}He^{2+}$. The output Twiss parameters are close to the matched ones at RFQ input (Table 1).

The $^{3}He^{++}$ beam transport, in comparison with the Deuteron one, required one more waist after the 3rd solenoid in order to reach the RFQ input Twiss parameters. As well as for Line 1, a good beam matching to the RFQ could be achieved for Line 2 for a wide range of input beam parameters.

4.3.2 RFQ

The Eurisol RFQ electromagnetic field distribution is similar to the SARAF RFQ one, except for the input radial matching section that was slightly modified. The standard profile used by the TOUTATIS code was adopted, with no significant change in performance. Simulation results for different ion species are presented in figs. 4.10 - 4.15 and in Table 4.1. No rms beam emittance growth was observed for the accelerated particles in the RFQ. Transmission efficiencies of 92%, 95% and 95% were obtained for H^{-}, D^{+} and $^{3}He^{++}$ beams, respectively.

Project funded by European Community under the "Structuring the European Research Area" Specific Programme Research Infrastructures Action within the 6th Framework Program (2002-2006)

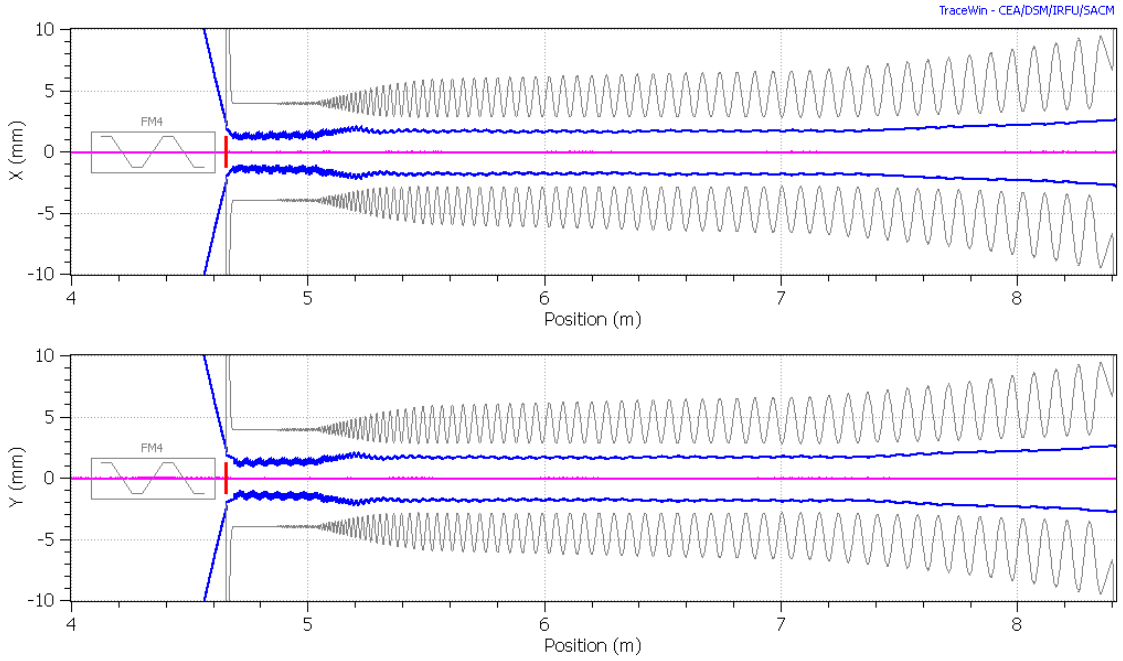

Fig. 4.10. H^- envelopes in the RFQ (2 rms).

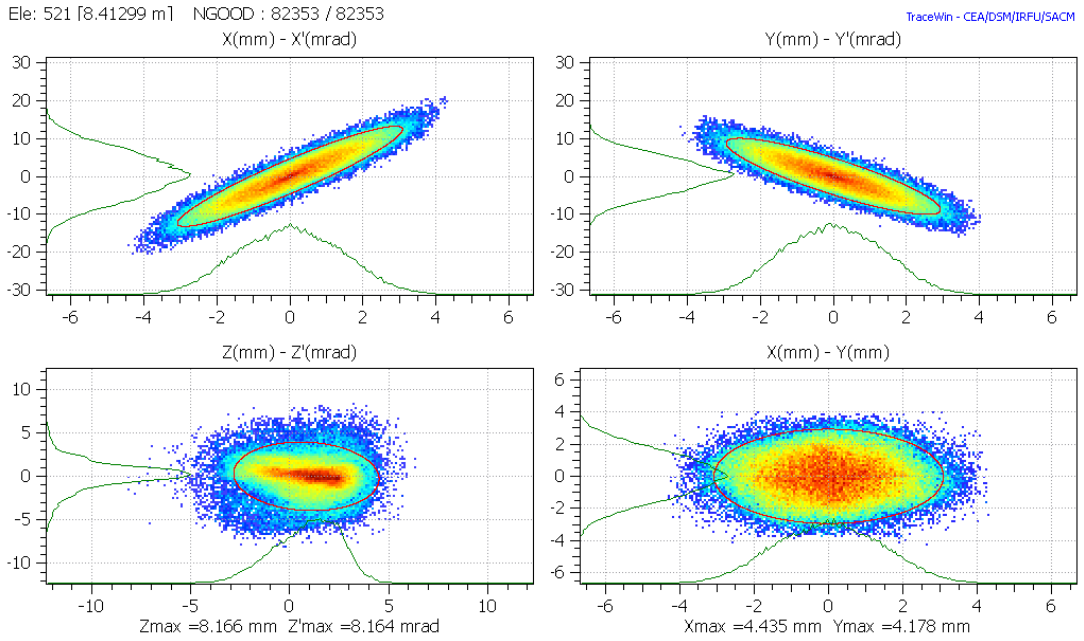

Fig. 4.11. H^- output phase spaces for the accelerated ions. 5 Rms emittance ellipses in red.

Project funded by European Community under the "Structuring the European Research Area" Specific Programme Research Infrastructures Action within the 6th Framework Program (2002-2006)

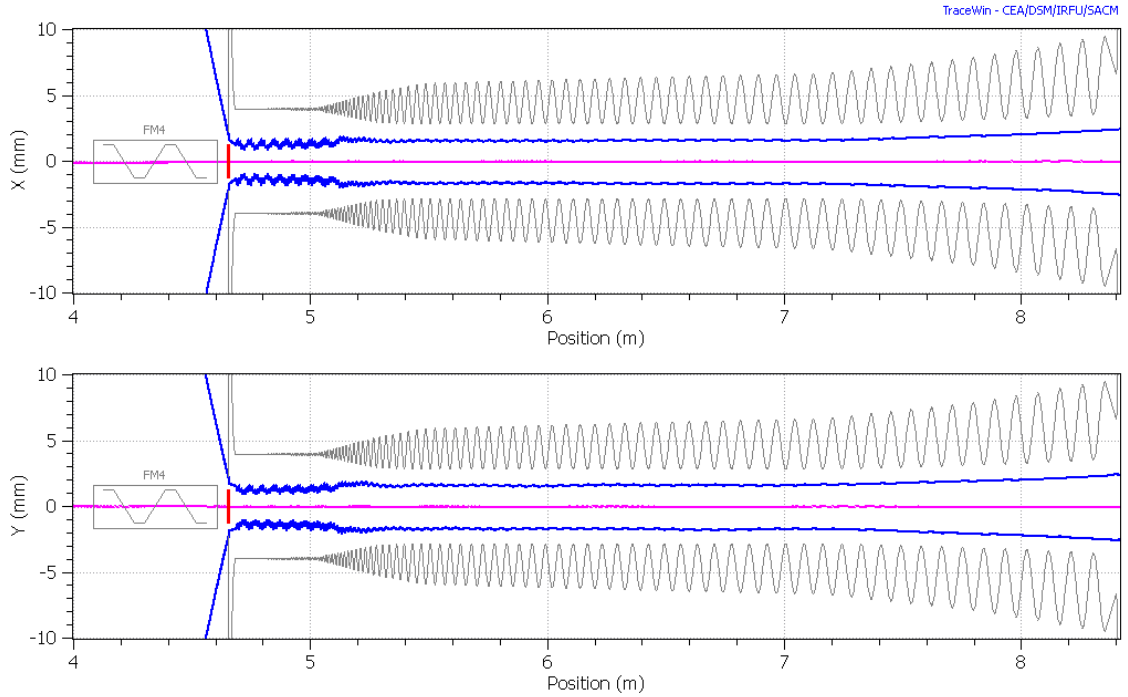

Fig. 4.12. Deuteron envelopes in the RFQ (2 rms).

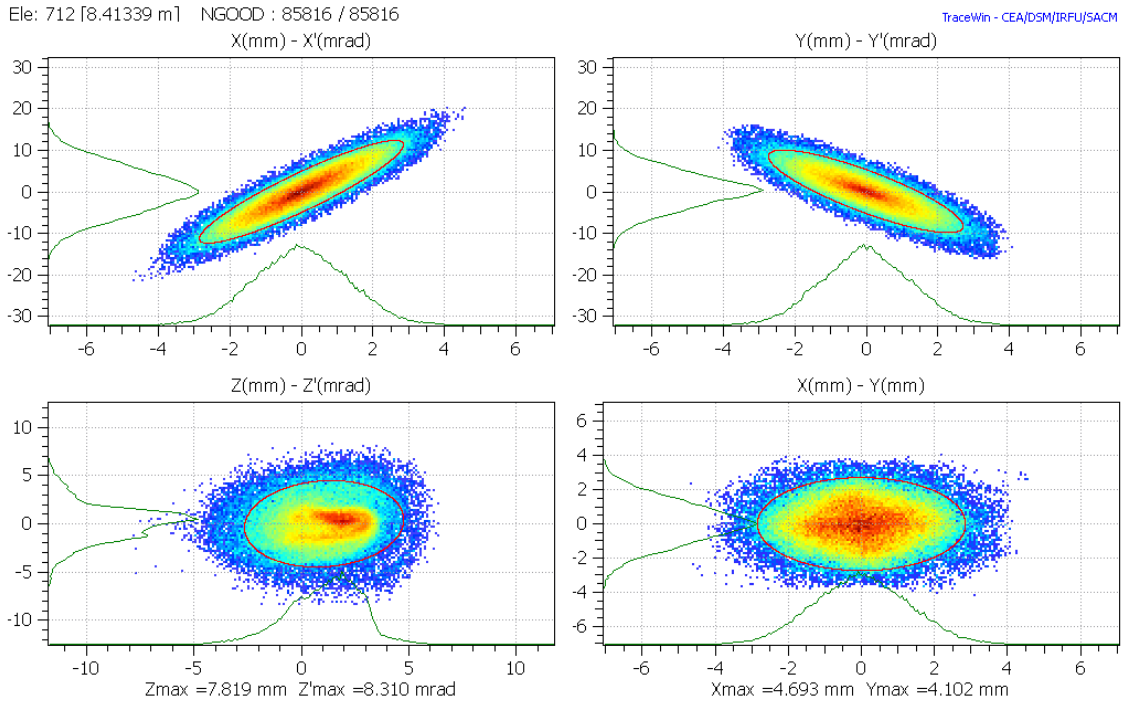

Fig. 4.13. Deuteron output phase spaces for the accelerated ions. 5 Rms emittance ellipses in red.

Project funded by European Community under the "Structuring the European Research Area" Specific Programme Research Infrastructures Action within the 6th Framework Program (2002-2006)

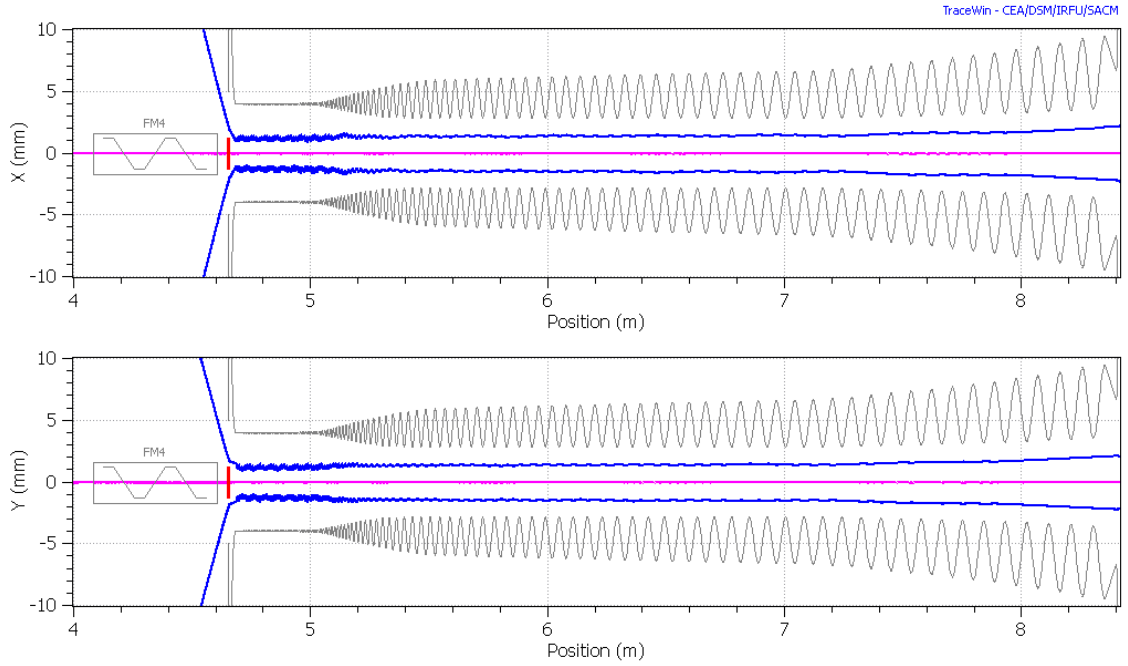

Fig. 4.14. $^{3}He^{2+}$ envelopes in the RFQ

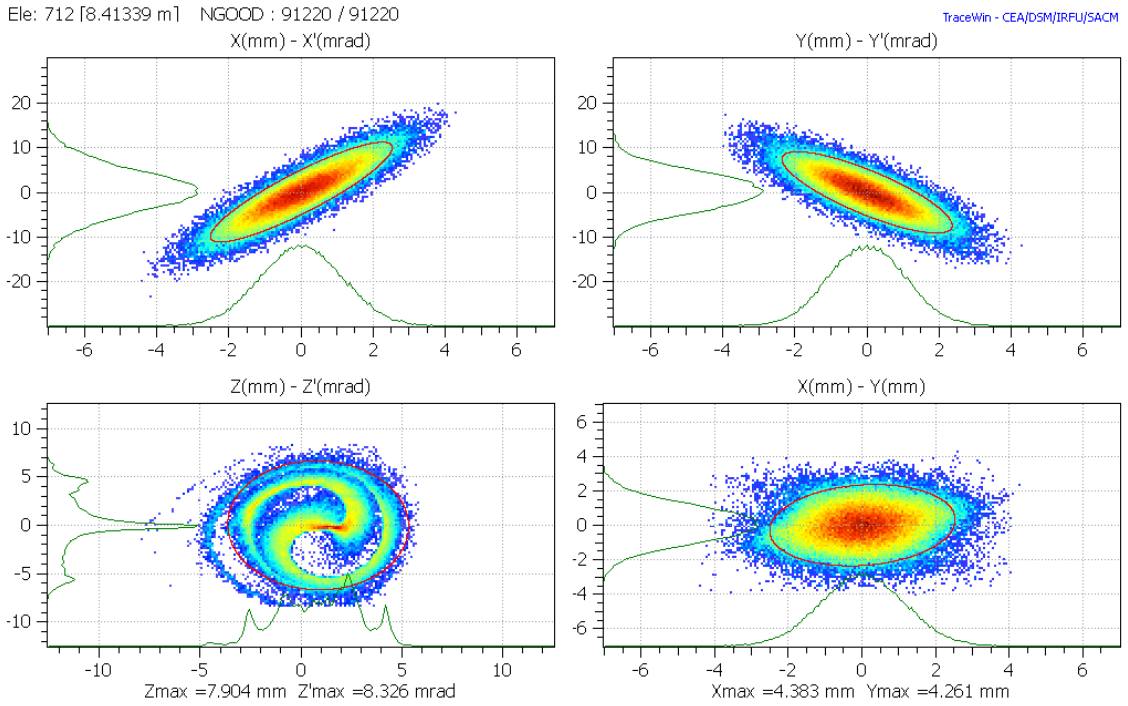

Fig. 4.15. $^{3}He^{2+}$ output phase spaces for the accelerated ions. 5 Rms emittance ellipses in red.

Project funded by European Community under the "Structuring the European Research Area" Specific Programme Research Infrastructures Action within the 6th Framework Program (2002-2006)

Table 4.1. Output beam parameters of the Ion Injector calculated with Partran-Toutatis.

Ions	W, MeV	W, MeV/u	I, mA	Beam rms emittance (π·mm·mrad)		
				$\varepsilon_{x,rms}$	$\varepsilon_{y,rms}$	$\varepsilon_{z,rms}$
H^-	1.5	1.5	5	0.16	0.16	0.16
D^+	3	1.5	5	0.15	0.15	0.18
$^3He^{2+}$	4.5	1.5	0.1	0.14	0.14	0.34

4.3.3 Beam losses

The IIS beam power losses, as shown by the beam dynamics simulations, are concentrated in the RFQ. The losses in the LEBT are mostly located at the diaphragm-suppressor. Although significant in terms of current, beam losses before the RFQ have very low power due to the low beam energy.

Particles transmitted, but not accelerated, in the RFQ have rather low energy and are almost completely filtered by the MEBT before reaching the low-β linac (see Deliverable D3). The IIS losses without errors are shown in Table 4.4.1. and in figures 4.4.1-3.

Table 4.2. Beam power losses and transmission along the IIS, for different beams. The RFQ transmission is listed both for accelerated particles and for all transmitted particles, including the not accelerated ones.

Ion Injector	H^-		D^+		$^3He^{++}$	
	Losses W	Transmission	Losses W	Transmission	Losses W	Transmission
LEBT	<1	98%	<1	99%	<1	98%
Diaphragm mm	12	91%	11	95%	0	100%
RFQ (accel.)	70	92%	90	95%	2	95%
RFQ (total)	-	96%	-	97%	-	98%

Project funded by European Community under the "Structuring the European Research Area" Specific Programme Research Infrastructures Action within the 6th Framework Program (2002-2006)

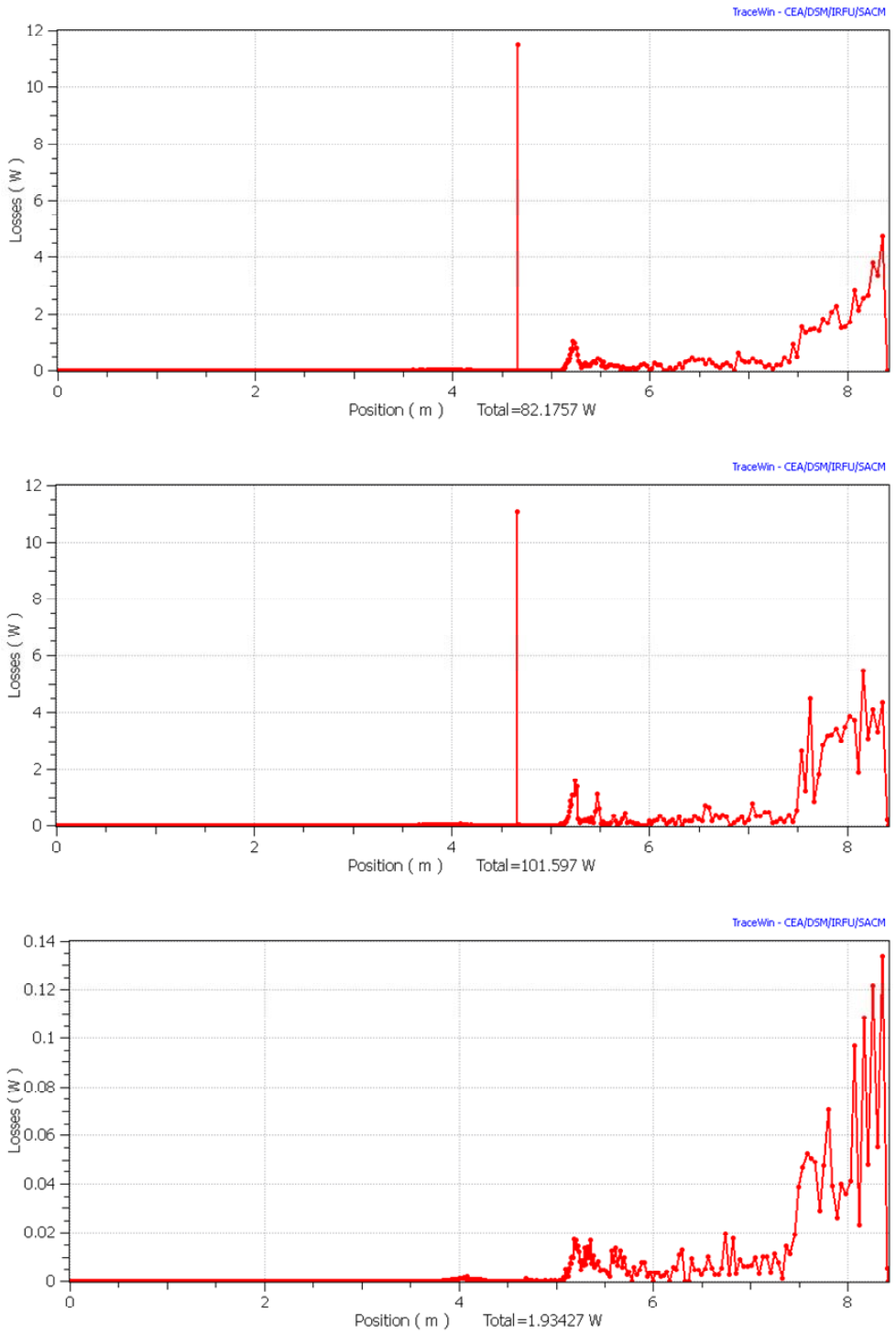

Fig. 4.16. Beam losses along Line 1 and RFQ. Top: H^-; middle: D+; bottom: $^3He^{2+}$. The peak at 4.66 m represents the power lost in the ∅=4.5 mm diaphragm before the RFQ.

Project funded by European Community under the "Structuring the European Research Area" Specific Programme Research Infrastructures Action within the 6th Framework Program (2002-2006)

Table 4.3. Maximum input errors considered in the LEBT-RFQ statistical study. In every run, the program generates a new set of random errors uniformly distributed in the range ±Δε, where Δε is the error value listed in the table.

type	error	unit	Source H-	Source D+	LEBT	RFQ
		Input beam				
Static	displacement X	mm	0.1	0.1		
	displacement Y	mm	0.1	0.1		
	displacement X'	mrad	0.1	0.1		
	displacement Y'	mrad	0.1	0.1		
	displacement Energy	MeV	1.00E-05	1.00E-05		
	ε_x increase	%	10	10		
	ε_y increase	%	10	10		
	ε_z increase	%	10	10		
	mismatch XX'	%	10	10		
	mismatch YY'	%	10	10		
	mismatch ZZ'	%	10	10		
	beam current	mA	0.5	0.5		
		Solenoid magnets				
static	displacement X	mm			0.1	
	displacement Y	mm			0.1	
	angle ϕ_x	deg			0.03	
	angle ϕ_y	deg			0.02	
	angle ϕ_z	deg			0.02	
	gradient	%			0.5	
	displacement Z	mm			1	
		RFQ electrodes (cell by cell)				
static	Long. Profile	mm				0.1
	Transv. curvature	mm				0.1
	gradient	%				1
		90° Dipole magnet				
static	displacement X	mm			0.1	
	displacement Y	mm			0.1	
	angle ϕ_x	deg			0.01	
	angle ϕ_y	deg			0.01	
	angle ϕ_z	deg			0.01	
	gradient	%			0.001	
	displacement Z	mm			0	

Project funded by European Community under the "Structuring the European Research Area" Specific Programme Research Infrastructures Action within the 6th Framework Program (2002-2006)

4.4 Preliminary error simulations

Error simulations of the LEBT-RFQ system were performed for H^-, D^+ and $^3He^{++}$ beams. Errors in a real linac are determined by the precision of the components alignment, by the errors in setting the fields in magnets, resonators, high voltage platforms, etc., by the stabilities of these fields (ripple, long term drifts, etc.), by the sensitivity of the beam diagnostics devices, and finally by the errors in the input beam. Errors can give a static (e.g. magnet misalignment) or a dynamic behavior (e.g. residual ripple of a power supply). The only automatic correction that we performed in the IIS simulation was the beam center position at the locations of beam position monitors (assumed sensitivity: 0.1 mm).

All errors are listed in table 4.3. Only dominant errors have been considered; some dynamic errors have been included in the static ones when treated in the same way by the simulation program (e.g. the error in the RFQ gradient, which has no correction in the simulation).

4.4.1 Tolerance determination

In this kind of search it is necessary to estimate the trend of the output beam changes versus the size of the input errors. Differently for the calculations of the beam losses distributions at high energy in the EURISOL driver, which come mainly from the halo particles and require a very large statistics to reach the required 1W/m sensitivity (see Deliverable D7-Beam loss calculations), this estimate is based on rms measurements of the beam distributions and could be done with lower statistics. We have used about 100000 macroparticles per point.

The search for acceptable tolerances was performed by simulating the errors up to their maximum value in 5 steps, in 50 runs with 5000 particles each. In every run the errors were randomly varied within the allowed error interval. The effects of misalignment were corrected in every run by means of steerers.

A final study, combining all errors, was then performed (see following graphs). The final errors resulting in the output beam (see Table 4.4) have been used as a starting point to set the errors of the input beam in the simulations of the following linac section (MEBT and low-β linac).

Project funded by European Community under the "Structuring the European Research Area" Specific Programme Research Infrastructures Action within the 6th Framework Program (2002-2006)

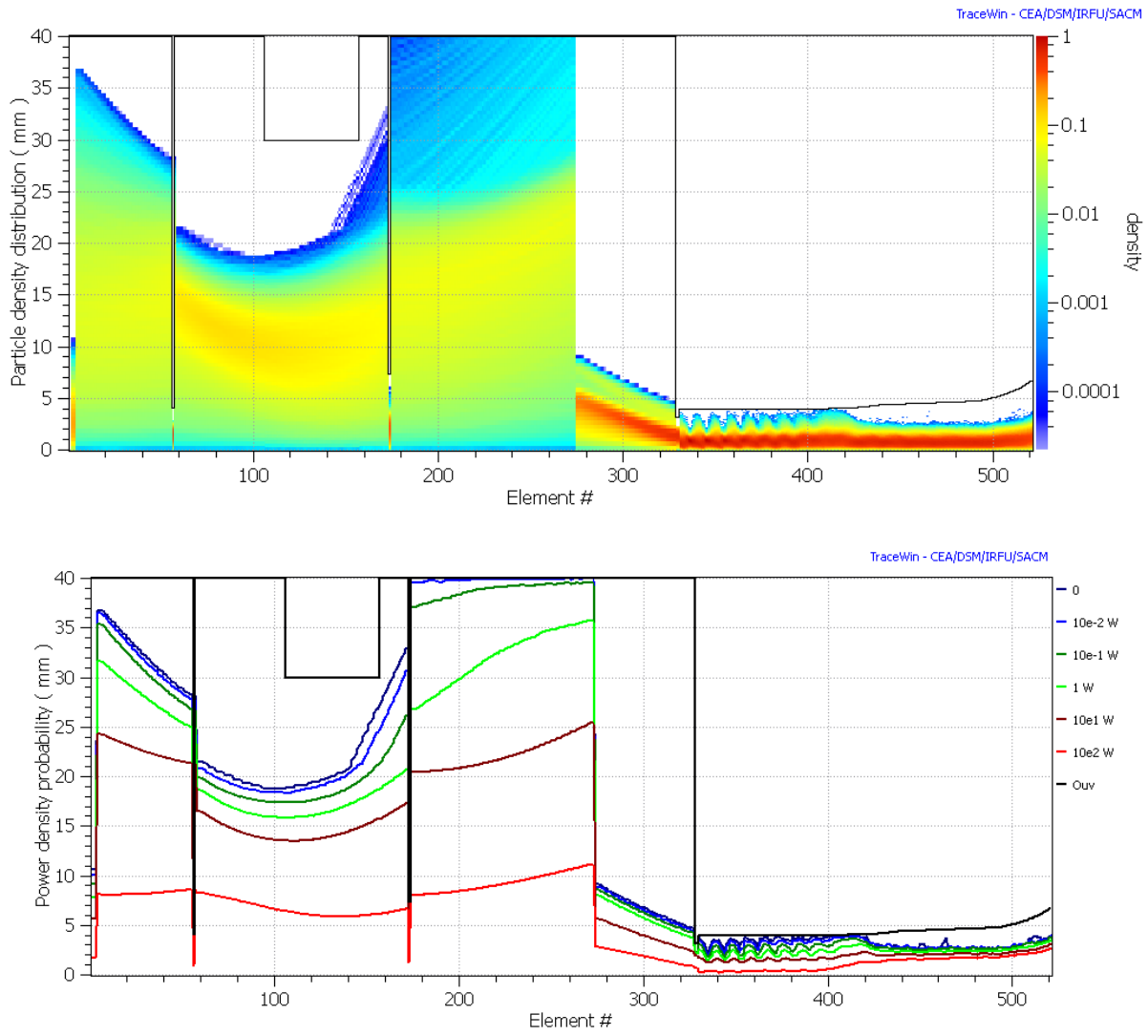

Fig. 4.17. H^- beam particle density (top) and power levels along the LEBT and RFQ, averaged over 20 runs, each one with 5000 macroparticles and a different set of errors uniformly distributed within the nominal limits.

Project funded by European Community under the "Structuring the European Research Area" Specific Programme Research Infrastructures Action within the 6th Framework Program (2002-2006)

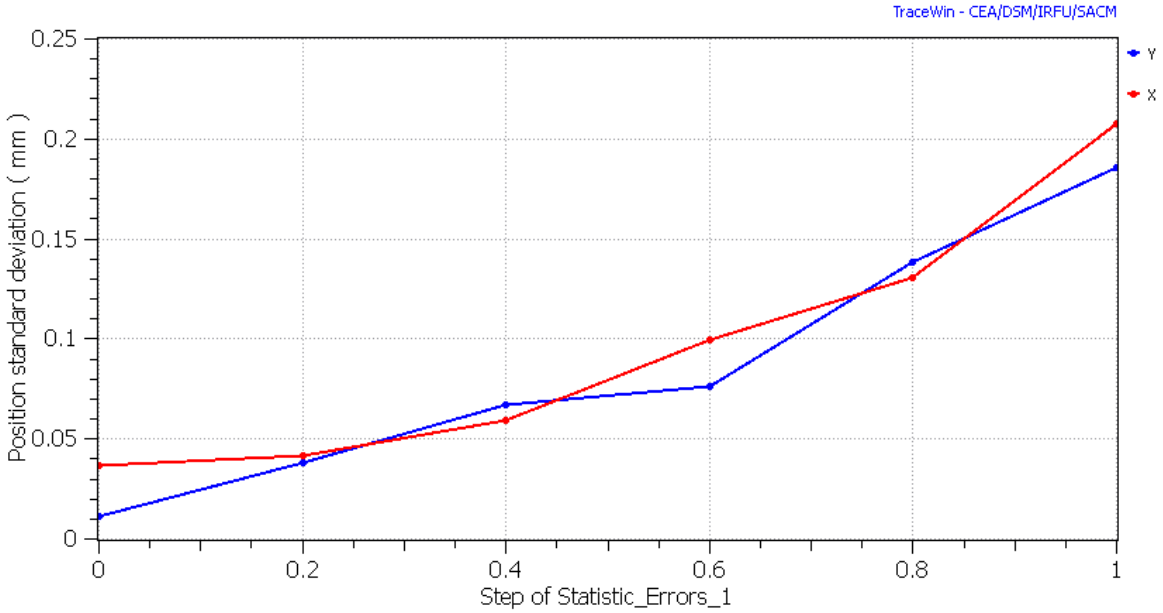

Fig. 4.18. Output H^- beam center position standard deviation as a function of the statistic errors (20 runs with 5000 macroparticles per point).

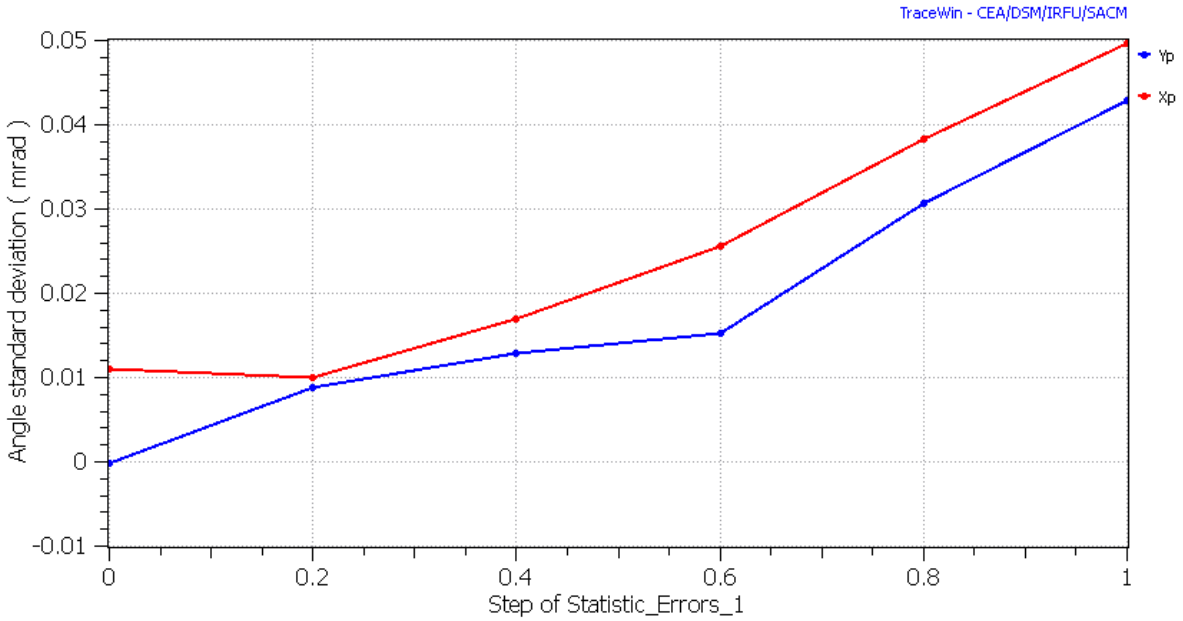

Fig. 4.19. Output H^- beam angle standard deviation as a function of the statistic errors (20 runs with 5000 macroparticles per point).

Project funded by European Community under the "Structuring the European Research Area" Specific Programme Research Infrastructures Action within the 6th Framework Program (2002-2006)

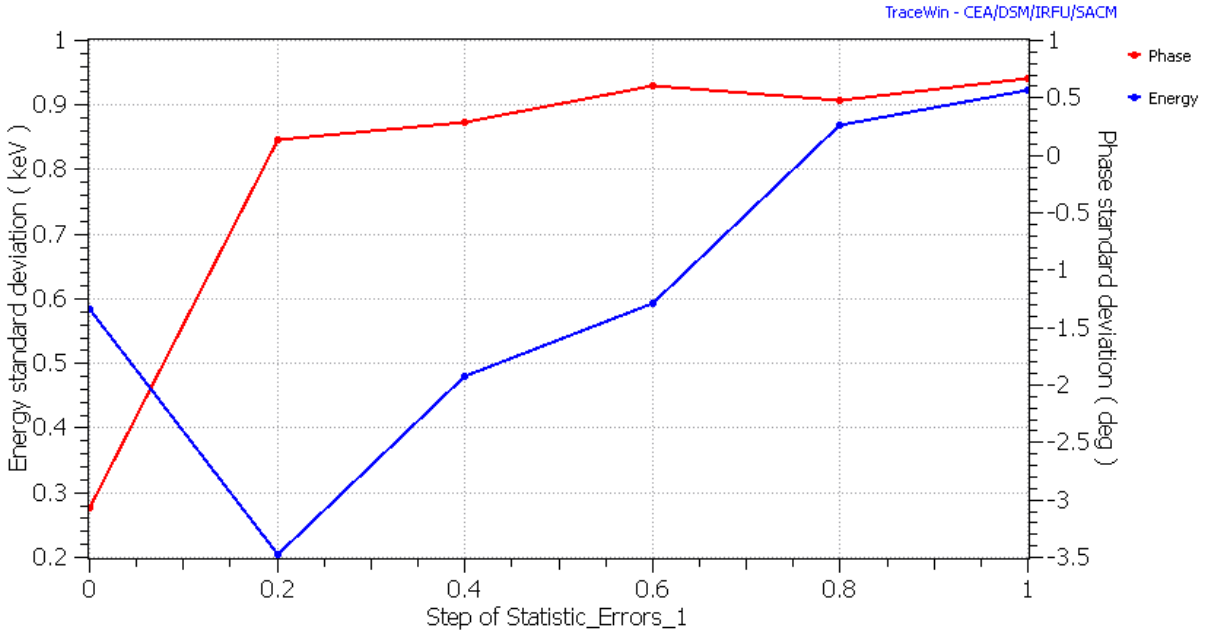

Fig. 4.20. Output H^- beam phase and energy standard deviation as a function of the statistic errors (20 runs with 5000 macroparticles per point).

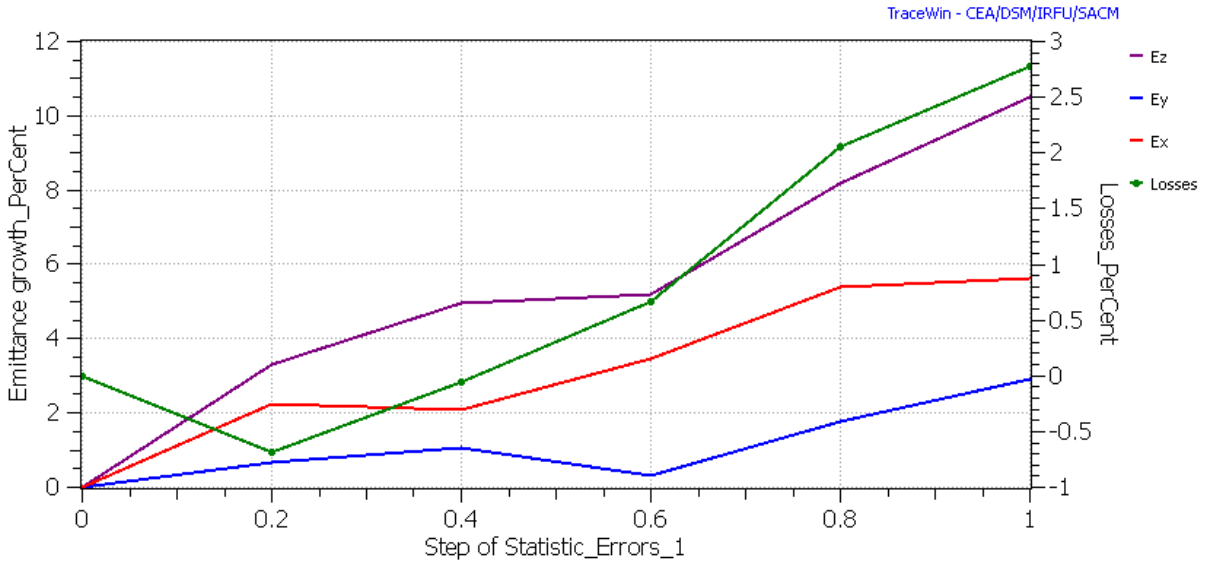

Fig. 4.21. Output H^- beam emittance growths and beam losses as a function of the statistic errors (20 runs with 5000 macroparticles per point).

Project funded by European Community under the "Structuring the European Research Area" Specific Programme Research Infrastructures Action within the 6th Framework Program (2002-2006)

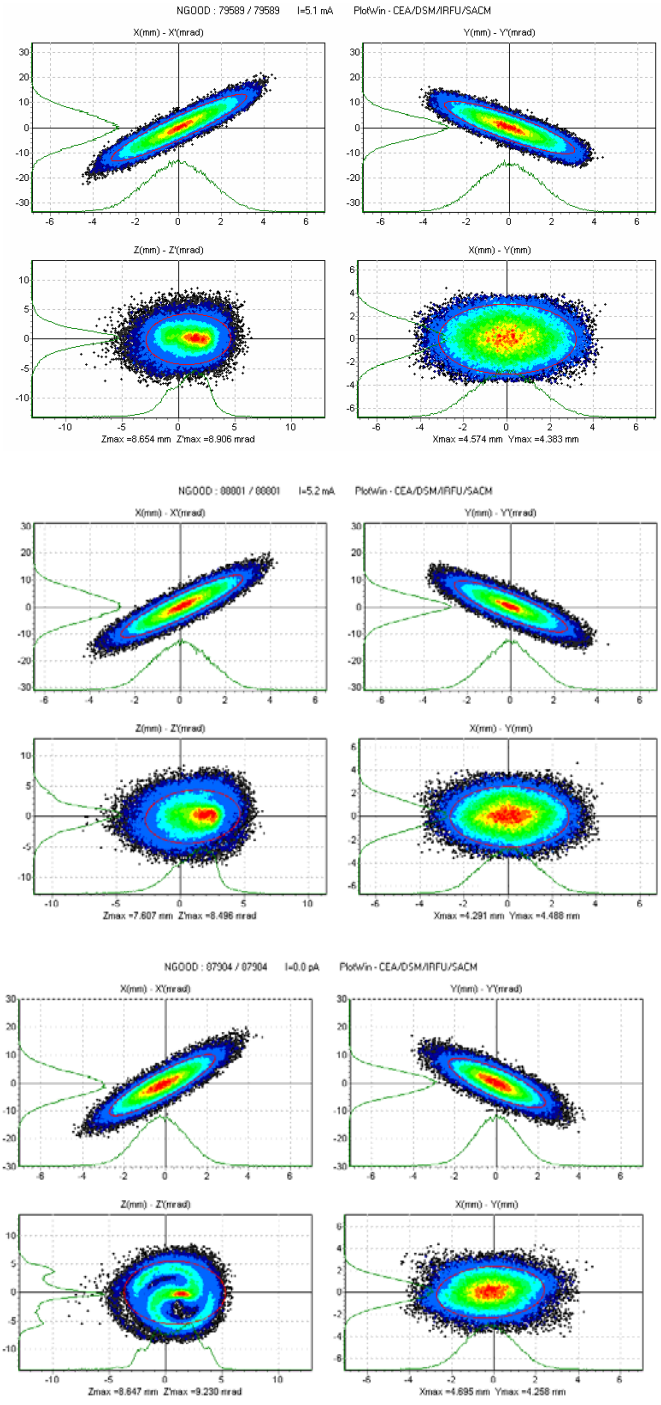

Fig. 4.22 Output H^-, D^+ and $^3He^{++}$ beam phase spaces, obtained by superimposing 20 runs with 5000 macroparticles (100000 macroparticles in total), each one with a different set of nominal errors.

Project funded by European Community under the "Structuring the European Research Area" Specific Programme Research Infrastructures Action within the 6th Framework Program (2002-2006)

Table 4.4. List of rms errors in the output beam, as a resul of the nominal errors applied to the input beam and to the LEBT-RFQ parameters. Calculation performed in 20 runs of 5000 macroparticles, each one with a different set of errors randomly distributed within the limits of Table 4.4, for a total number of 100000 particles.

Error type	symbol	unit	Output beam error (rms)		
			H^-	D^+	$^3He^{++}$
Position x	δx	*mm*	0.21	0.18	0.16
Position y	δy	*mm*	0.19	0.15	0.13
Phase	$\delta\phi$	*deg*	0.7	0.3	0.7
Angle x	$\delta x'$	*mrad*	0.05	0.04	0.04
Angle y	$\delta y'$	*mrad*	0.04	0.04	0.03
Energy	δE	*keV/u*	0.9	0.7	0.9
Emittance growth x	$\delta\varepsilon_x$	*%*	6	3	3.3
Emittance growth y	$\delta\varepsilon_y$	*%*	3	4	0.6
Emittance growth z	$\delta\varepsilon_z$	*%*	10	5	1.6

Project funded by European Community under the "Structuring the European Research Area" Specific Programme Research Infrastructures Action within the 6th Framework Program (2002-2006)

5. Injector Operation modes

The IIS design must take into account not only the steady state configuration, but also the different configurations that are required in the accelerator commissioning and operation, and also in case of situations which require an emergency procedure (e.g. failure of some components, radiation above allowed limits, etc.).

The main configurations considered are 1) beam set-up; 2) beam shut down; 3) steady state cw operation.

5.1 Beam set-up

The beam set-up requires turning on of the linac elements in sequence and verification of the effect of every action by means of diagnostic elements. The beam set-up of the Sources and LEBT can be done in cw mode, since the maximum beam power before the RFQ is a few hundreds Watts of 20 keV/A particles. The beam can be stopped in the water-cooled Faraday cup or in the switched-off RFQ.

When the RFQ is switched on, the beam power reaches 7.5 kW in cw mode. In order to avoid large beam power losses during the set-up phase, a pulsed beam is used, reducing the average current by orders of magnitude but not the nominal current inside the pulse, which is at the origin of the space charge forces. The pulse length must be sufficiently long to allow steady space charge compensation, which is strongly dependent on vacuum level and typically of the order of 10 µs for H^- in operation conditions [7].

The beam can be pulsed by simply pulsing both the RFQ rf power and the beam source. The typical time required to the ECR source to reach the full current is about 200 µs, and its decay time is about 20 µs. The RFQ rise- and decay-time is of the same order. To produce a sharp pulse, the source is switched on while the RFQ is at 10% voltage; after 200 µs the RFQ voltage is raised to 100% and the pulse is transmitted with a risetime of µs. The pulse stops with the shut down of the source, with a typical decay time of 20 µs. The pulse length is given by the delay between RFQ switch on and source switch off.

5.2 Steady state cw

The cw operation is reached, after setting up completely the pulsed beam, by deactivating the pulsing

Project funded by European Community under the "Structuring the European Research Area" Specific Programme Research Infrastructures Action within the 6th Framework Program (2002-2006)

system.

5.3 Beam shut down (normal and emergency)

The beam can be shut down by means of the following actions:

a) Switch off of the ion source. This stops the beam in ~20 μs.

b) Insertion of the beam stopper before the bending dipole. This mechanical operation requires milliseconds to be completed.

c) Switch off of the RFQ rf power (~20 μs) to stop the beam before the linac.

d) Insertion of the Faraday cup for beam current measurement. This operation requires approximately ~1 s.

Emergency beam shut down can be done in about 20 μs by switching off the source and the RFQ, and by inserting the beam stopper.

5.4 Beam losses in startup, shutdown and emergency conditions

Beam losses in normal operation are reported in par. 4.7. The maximum beam power at the RFQ injection is 200 W. In the pulsed beam operation, when the RFQ is shut down and its voltage drops well below the nominal operation value, particles are nor accelerated nor focused anymore for a few microseconds, being lost mainly inside the RFQ. The location of these time dependent losses cannot be calculated precisely, but their total amount is negligible due to the low duty cycle (about 0.1%). In case of failure of some components, the fast shutdown procedure will be started, with switch-off of th RFQ and of the ion source. Losses location will depend on the type of failure. The total deposited energy is going to be about $P\cdot(\tau_1+\tau_2)$, where P is the beam power, τ_1 is the time required for the control system to detect the failure and to give the fast shutdown command, and τ_2~ is the time required by the ion source and the RFQ to switch off the beam.

Project funded by European Community under the "Structuring the European Research Area" Specific Programme Research Infrastructures Action within the 6th Framework Program (2002-2006)

6. Conclusions

The layout of the EURISOL Driver linac Ion Injector was designed and its beam dynamics was studied in detail. The maximum allowable errors in the construction and in the operation parameters have been assessed. This injector allows to produce and accelerate H-, D+, 3He++, H+, H2+ ions required for the EURISOL driver operation. Although the double capability of positive and negative ions is not common, this accelerator section has been designed having in mind reliability in construction time and operation. The main accelerator components, where possible, have been chosen among existing devices in order to minimise risks connected to R&D programs.

The layout resulting from the present study allows to meet all requirements of the EURISOL injector.

Project funded by European Community under the "Structuring the European Research Area" Specific Programme Research Infrastructures Action within the 6th Framework Program (2002-2006)

7. References

[1] A. Facco, A. Balabin, R. Paparella, D. ZenereD. Berkovits, J. Rodnizki, J. L. Biarrotte, S. Bousson, A. Ponton, R. Duperrier, D. Uriot, V. Zvyagintsev, “BEAM DYNAMICS STUDIES ON THE EURISOL DRIVER ACCELERATOR”, Proc. of LINAC08, Vancouver, Canada, 2008.

[2] K. Dunkel et al., "Performance of the SARAF Ion Source", PAC'07, Alboquerque, June 2007, TUPAN009, p. 1407 (2007).

[3] P. Fischer, A. Schempp and J. Haeuser, ”A CW RFQ ACCELERATOR FOR DEUTERONS”, PAC’05, May 2005, Knoxville, Tennessee, USA, p.794, and P.Fischer, A.Schempp “Tuning of a 4-rod cw-mode RFQ accelerator”, EPAC’06, Edinburgh, (June, 2006).

[4] T. Kuo, D. Yuan, K. Jayamanna, M. McDonald, R. Baartman, W. Z. Gelbart, N. Stevenson, P. Schmor, and G. Dutto, Rev. Sci. Instr. Vol.69 N.2, February 1998.

[5] C.Piel et al. “Development and performance of a proton and deuteron ion source”, PAC’05, Knoxville, 2005

[6] R. Baartman and D. Yuan, Proc. of EPAC 1988, p. 949.

[7] Ahmed Ben Ismail, Romuald Duperrier, Didier Uriot, Nicolas Pichoff, Proceedings of HB2006, Tsukuba, Japan, p. 187.

[8] R. Duperrier et al., Proc. of EPAC04, p. 2023.

[9] E. Fagotti, "SPES LEBT: electron trap device", LNL 2003 Annual report, E124TT, http://www.lnl.infn.it/~annrep/read_ar/2003/pdfs_2003/E124TT.pdf

[10] P.Fischer, A.Schempp, Proc. of EPAC 2006, p. 1583; P. Fischer, A. Schempp and J. Haeuser, Proc. of PAC’05, p.794.

[11] R. Duperrier, N. Pichoff, and D. Uriot, in Proceedings of the International Conference Computational Science, Amsterdam, 2002.

[12] T. Taylor and J. F. Mouris, Nucl. Instrum. Methods A 336, 1 (1993).

[13] Florian Kremer, Kai Dunkel and Christian Piel, "Performance of the SARAF ECR Ion Source", presented in ICIS 2007 the 12th International Conference on Ion Sources 26-31 Aug 2007, Jeju, South Korea

[14] K.-H. Schmidt, A. Kelic´, S. Lukic´, M.V. Ricciardi, and M. Veselsky, Phys. Rev. ST Accelerators and Beams, 10, 014701 (2007)

[15] A. Pisent et al., “IFMIF-EVEDA RFQ DESIGN”, proc. of EPAC08, Genoa, Italy, p. 3542.

[16] D. Schrage et al., “A 6.7-MEV CW RFQ LINAC”, proc. of PAC97, Vancouver, Canada, p. 1093.

[17] A. Pisent et al., “The TRASCO-SPES RFQ”, proc. of LINAC 2004, Lubeck, Germany, p. 69.

[18] R.F. Welton, “OVERVIEW OF HIGH-BRIGHTNESS H ION SOURCES”, proc. of LINAC 2002, Gyeongyu, Korea, p. 559.

[19] Chauvin et al, “BEAM DYNAMICS SIMULATIONS OF THE LOW ENERGY BEAM TRANSPORT LINE FOR IFMIF-EVEDA ” proc. of LINAC’08, Vancouver, Canada, p. 241

[20] R. Ferdinand et al., Proc. of PAC 1997, p. 2723.

Project funded by European Community under the “Structuring the European Research Area” Specific Programme Research Infrastructures Action within the 6th Framework Program (2002-2006)